

# Echocardiographic Imaging for Transcatheter Aortic Valve Replacement



Rebecca T. Hahn, MD, Alina Nicoara, MD, Samir Kapadia, MD, Lars Svensson, MD, PhD,  
and Randolph Martin, MD,

*New York, New York; Durham, North Carolina; Cleveland, Ohio; and Atlanta, Georgia*

---

Transcatheter aortic valve replacement has become an accepted alternative to surgery for patients with severe, symptomatic aortic stenosis who are inoperable or are at high surgical risk. Recent trials support the use of transcatheter aortic valve replacement also in patients at intermediate risk, and ongoing trials are assessing appropriateness in other patient groups. The authors review the key anatomic features integral to the transcatheter aortic valve replacement procedure and the echocardiographic imaging required for preprocedural, intraprocedural, and postprocedural assessment. (*J Am Soc Echocardiogr* 2018;31:405-33.)

**Keywords:** Aortic stenosis, Transcatheter aortic valve replacement, Echocardiography

---

Transcatheter aortic valve replacement (TAVR) is now a class I recommendation for treatment of prohibitive-risk and high-surgical risk patients with severe, symptomatic aortic stenosis (AS).<sup>1</sup> TAVR currently has a class IIa recommendation for patients at intermediate surgical risk, but given the large randomized trials showing noninferiority to surgical aortic valve replacement, TAVR may be an appropriate alternative in this population as well.<sup>2,3</sup> TAVR volumes continue to increase as indications for use expand.<sup>4,5</sup> In this article, we review the anatomic features integral to the TAVR procedure and the echocardiographic imaging required for preprocedural, intraprocedural, and postprocedural assessment.

## ANATOMIC PERSPECTIVE

---

Characterization of the aortic root complex, consisting of the aortic valve, aortic annulus, sinuses of Valsalva, and sinotubular junction, is critical for planning and success of TAVR. The normal aortic valve has three leaflets supported by the aortic sinuses: left, right, and noncoronary. The right coronary leaflet rests on the muscular part of the interventricular septum, the noncoronary leaflet is adjacent to the membranous septum and the anterior

mitral leaflet, and the left coronary leaflet is continuous with the anterior mitral leaflet (aortomitral curtain) and muscular interventricular septum (Figure 1).<sup>6</sup> Between the semilunar hinge lines of the leaflets are the fibrous interleaflet trigones or triangles.<sup>7</sup> The anatomic aortic annulus is defined as the semilunar lines of attachment of the aortic valve leaflets to the aortic sinuses. However, measurement of the aortic annulus relevant to transcatheter heart valve (THV) sizing is performed at the most ventricular (basal) hinge points of the leaflets, referred to as the ventricular ring. More than half the circumference of this ring is formed by the base of the interleaflet triangles; this plane is thus the “virtual” annulus. The coronary arteries arise at a variable distance from the base of left and right coronary cusps.<sup>8</sup> The left coronary ostium is frequently in the posterior part of the left sinus, and the right coronary ostium is somewhat anterior and superior in the right sinus. The lower position of the left coronary increase its risk for obstruction by a calcified aortic leaflet.<sup>9</sup> Also, the atrioventricular bundle then courses on the top of the muscular septum under the membranous septum, where it divides into the left and right bundles (Figure 1) and thus is at risk for damage with TAVR depending in part on the depth of THV implantation.<sup>10,11</sup> The atrioventricular bundle then courses on the top of the muscular septum under the membranous septum.

One important anatomic variation is the bicuspid aortic valve, which was an exclusion criterion for early TAVR trials<sup>12,13</sup> and may be associated with worse procedural outcomes compared with trileaflet valves.<sup>14,15</sup> Anatomic differences compared with the trileaflet valve include a larger and more circular annulus, larger sinus of Valsalva and ascending aorta, and more eccentric annular calcification,<sup>16</sup> which may contribute to greater degrees of post-TAVR paravalvular aortic regurgitation (PAR)<sup>15,17</sup> and a higher incidence of post-TAVR conduction abnormalities.<sup>18</sup> The Bicuspid TAVR Registry has recently shown good success rates in these patients using new-generation transcatheter valves.<sup>19</sup> Improved preprocedural sizing using multislice computed tomography (MSCT)<sup>15</sup> as well as implantation techniques may mitigate these complications. Bicuspid valves were classified by Sievers and Schmidtke<sup>20</sup> as type 0, no raphe;

---

From Columbia University Medical Center, New York, New York (R.T.H.); Duke University Medical Center, Durham, North Carolina (A.N.); Cleveland Clinic, Cleveland, Ohio (S.K., L.S.); and Emory University, Atlanta, Georgia (R.M.).

Conflicts of Interest: Dr. Hahn is the Cardiovascular Research Foundation echocardiography core laboratory director for a number of trials, including the PARTNER trial, for which she receives no direct compensation.

Reprint requests: Rebecca T. Hahn, MD, Columbia University Medical Center, New York-Presbyterian Hospital, 177 Fort Washington Avenue, New York, NY 10032 (E-mail: [rth2@columbia.edu](mailto:rth2@columbia.edu)).

0894-7317/\$36.00

Copyright 2017 by the American Society of Echocardiography.

<https://doi.org/10.1016/j.echo.2017.10.022>

**Abbreviations**

<b>2D</b> = Two-dimensional
<b>3D</b> = Three-dimensional
<b>ACC</b> = American College of Cardiology
<b>AHA</b> = American Heart Association
<b>AS</b> = Aortic stenosis
<b>AVA</b> = Aortic valve area
<b>BSA</b> = Body surface area
<b>CS</b> = Conscious sedation
<b>EF</b> = Ejection fraction
<b>ELI</b> = Energy loss index
<b>GA</b> = General anesthesia
<b>GLS</b> = Global longitudinal strain
<b>HR</b> = Hazard ratio
<b>LV</b> = Left ventricular
<b>LVOT</b> = Left ventricular outflow tract
<b>MR</b> = Mitral regurgitation
<b>MSCT</b> = Multislice computed tomography
<b>PAR</b> = Paravalvular aortic regurgitation
<b>PARTNER</b> = Placement of Aortic Transcatheter Valves
<b>TAVR</b> = Transcatheter aortic valve replacement
<b>TEE</b> = Transesophageal echocardiography
<b>THV</b> = Transcatheter heart valve
<b>TR</b> = Tricuspid regurgitation
<b>TTE</b> = Transthoracic echocardiography
<b>VARC</b> = Valve Academic Research Consortium
<b>Z<sub>va</sub></b> = Valvuloarterial impedance

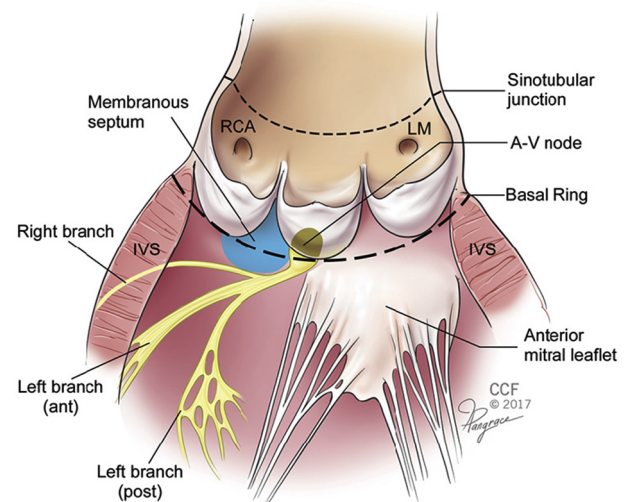
type 1, with one raphe (most commonly seen between the left and right coronary cusps); and type 2, with two raphes. Type 1 bicuspid aortic valve anatomy with left and right cusp fusion may have better post-TAVR outcomes compared with other anatomic variants.<sup>21</sup>

### PREPROCEDURAL IMAGING WITH ECHOCARDIOGRAPHY

The current American Heart Association (AHA)/American College of Cardiology (ACC) and European Association of Cardiovascular Imaging valvular heart disease guidelines<sup>1,22</sup> discuss the importance of the heart team approach to the management of complex valvular heart disease. An important part of that team is the cardiovascular imaging specialist. Throughout the development of the TAVR procedure for severe, symptomatic AS, echocardiographic imaging has played an essential role in the preprocedural assessment of patients, intraprocedural guidance, and postprocedural follow-up.<sup>23,24</sup> As indications for both surgical aortic valve replacement and TAVR continue to evolve,<sup>1</sup> echocardiography may play an even more important role in patient diagnosis and management. In this section we review the role of echocardiography in the selection of patients for TAVR.

#### Morphology of the Aortic Valve

Distinguishing bicuspid from tricuspid aortic valve is essential before TAVR. Although multiple imaging modalities can assess the morphology of the aortic valve and root, the diag-



**Figure 1** Conduction system. The aortic valve node is typically located on the floor of the right atrium just posterior (post) and inferior to the membranous septum (blue shaded region). The atrioventricular (A-V) node and bundle then courses on the top of the muscular septum under the membranous septum, where it divides into the left and right bundles. *ant*, Anterior; *IVS*, interventricular septum; *LM*, left main coronary artery; *RCA*, right coronary artery.

uncertainty may remain in 10% to 15% of patients after echocardiography.<sup>27</sup> In the setting of calcification with reduced leaflet excursion in systole, the abnormal motion of the two cusps may not be appreciated, and color Doppler may be helpful in distinguishing immobile trileaflet aortic valves without commissural fusion from bicuspid valves with fusion; color Doppler flow in all three commissures should be seen with trileaflet valves.<sup>28</sup>

In addition to determining the number of cusps, the location and severity of calcium are important aspects of morphologic assessment. The prognostic importance of valve calcium by echocardiography has long been recognized,<sup>29,30</sup> but MSCT has become the primary imaging modality for quantification of calcium burden.<sup>31-33</sup> Ectopic calcification of the left ventricular outflow tract (LVOT) is predictive of PAR.<sup>34,35</sup> In addition, in patients with low flow, the severity of calcification may help distinguish those patients with true severe AS from those patients with pseudosevere AS.<sup>36-38</sup> Sex-specific criteria have been established, with aortic valve calcium cutoffs for severe AS of  $\geq 1,275$  arbitrary units in women and 2,065 arbitrary units in men. Interestingly, aortic valve calcium is also lower in women after indexing to body size or annular area,<sup>37,39</sup> consistent with findings of increased fibrosis in women.<sup>40</sup>

#### Assessment of Severity of AS

Echocardiography is used to assess valve morphology and severity of stenosis, as well as the cardiac response to AS, including left ventricular (LV) remodeling and function, mitral valve regurgitation, and pulmonary hypertension. Recent updates to the American Society of Echocardiography and European Society of Echocardiography guidelines,<sup>41</sup> as well as an associated letter to the editor,<sup>42</sup> review the echocardiographic parameters and acquisition recommendations. These parameters can be divided into flow-dependent measurements and flow-independent measurements and are summarized in Table 1.

nosis of bicuspid aortic valve is typically made using echocardiography. The short-axis views of the valve in systole should image a typical “fish-mouth” appearance of valve opening and absence of opening at the raphe. Systolic doming from the long-axis view may be another clue of a bicuspid valve. In patients with good-quality transthoracic images who do not have dense calcification, diagnostic sensitivity and specificity for identification of a bicuspid valve are >70% and >90%, respectively,<sup>25,26</sup> but diagnostic

The greatest error in the aortic valve area (AVA) calculation is the squared LVOT diameter measurement. There are important caveats about the measurement of the LVOT diameter in the setting of AS (Figure 2, Table 2).

- LVOT diameter should be measured at early to mid-systole (when the elliptical LVOT is more circular) from the image that provides the largest diameter.<sup>43</sup>
- LVOT diameter should be measured from the inner edge to inner edge from where the anterior (right coronary) cusp meets the ventricular anterosseptum, to the posterior “virtual annulus” where the posterior interleaflet triangle meets the anterior mitral leaflet.<sup>44</sup> Avoid measuring the ectopic calcium as a border of the LVOT.
- LVOT diameter measured below the aortic annulus underestimates catheter-derived AVA.<sup>43,45</sup> This may be particularly true in the setting of a sigmoid septum.
- AVA calculated with LVOT diameter measured at the level of the aortic annulus is more accurate and reproducible.<sup>45-47</sup>
- Because the greatest error in AVA calculation is the squared LVOT diameter measurement, using the ratio of  $V_{LVOT}/V_{AS}$  jet or  $VTI_{LVOT}/VTI_{aortic\ valve}$  can be a good indicator of AVA. A Doppler velocity index of  $\leq 0.25$  indicates severe stenosis.

Although echocardiographic guidelines recommend a single diameter measurement of the LVOT to calculate AVA, planimetry of the aortic valve and LVOT area by real-time three-dimensional (3D) methods has been shown to be accurate and reproducible<sup>48,49</sup> and to compare favorably with MSCT.<sup>50,51</sup> Some studies suggest that using a direct area measurement of the LVOT in the continuity equation may yield a more accurate measurement of AVA.<sup>52,53</sup> However, Clavel *et al.*<sup>54</sup> compared the two methods for calculating AVA: the hybrid multislice computed tomographic planimetric LVOT in the continuity equation and the standard echocardiographic continuity equation. Compared with echocardiographic AVA, the hybrid method did not improve the correlation with transvalvular gradient, concordance between gradient and AVA, or prediction of mortality. Importantly, thresholds for excess mortality differed between techniques:  $AVA \leq 1.0\text{ cm}^2$  for the echocardiographic method versus  $\leq 1.2\text{ cm}^2$  for the hybrid method. These findings and other outcomes studies using the echocardiographic method for calculating AVA<sup>54,55</sup> support the continued use of standard linear LVOT dimension to measure AVA and to guide management as recommended by current guidelines.<sup>1</sup>

Because small-sized patients may not require the same amount of cardiac output as larger patients, the American Society of Echocardiography recommends indexing the valve area to body surface area (BSA), particularly in smaller patients with height < 135 cm (65 in),  $BSA < 1.5\text{ m}^2$ , or body mass index < 22  $\text{kg}/\text{m}^2$ . The ACC guidelines use an indexed AVA of  $\leq 0.6\text{ cm}^2/\text{m}^2$  to define severe AS. Importantly, indexing to BSA may not be appropriate in obese patients.<sup>41</sup>

Some investigators have suggested that using an indexed cut-off of  $< 0.5\text{ cm}^2/\text{m}^2$  may not only reduce inconsistent measurements with unindexed values,<sup>47,56</sup> but lower indexed AVA cut-offs may also improve the prediction of outcomes.<sup>56,57</sup>

### Low-Gradient, Severe AS

As many as 40% of patients with AS may have discordant Doppler hemodynamics with low mean gradient (<40 mm Hg) in the setting of severely reduced valve area ( $\leq 1.0\text{ cm}^2$ ). Many of these patients have low flow, currently defined as a stroke volume index of  $< 35\text{ mL}/\text{m}^2$ . Current AHA/ACC guidelines have subdivided the se-

## HIGHLIGHTS

- The imager is an essential member of the Heart Team for the TAVR procedure.
- Echocardiography is the imaging modality of choice for the assessment of aortic valve morphology and function.
- Echocardiography is a valuable adjunctive imaging modality for planning prior to transcatheter aortic valve replacement.
- Echocardiography is an essential imaging tool for intraprocedural guidance and postprocedural assessment of transcatheter aortic valve replacement.

vere, symptomatic AS group of patients (stage D) into three separate categories: high-gradient AS (stage D1); low-flow, low-gradient AS with reduced ejection fraction (EF; stage D2); and low-gradient AS with normal EF (stage D3). Figure 3 shows the suggested approach to these subgroups of severe symptomatic AS.

Classic low-flow, low-gradient (mean gradient < 40 mm Hg) AS ( $AVA \leq 1\text{ cm}^2$ ) with reduced EF (<50%; stage D2 in the ACC/AHA guidelines) is often associated with coronary artery disease but may have intrinsic disease of the myocardium or afterload mismatch related to severe stenosis. Because valve area has been shown to be flow dependent,<sup>59,60</sup> multiple studies have used low-dose dobutamine stress echocardiography to increase the transvalvular flow rate while avoiding myocardial ischemia.<sup>61-65</sup> The protocol for this test is described in the American Society of Echocardiography updated guidelines.<sup>41</sup>

The D3 category of low-gradient, severe AS with normal EF is also known as “paradoxical AS.” Because velocity and gradient are dependent on flow, a number of physiologic situations can result in low flow in the setting of normal EF: tachycardia,<sup>66</sup> bradycardia,<sup>67</sup> hypertension,<sup>68-70</sup> small ventricular cavity,<sup>71</sup> severe diastolic dysfunction, severe mitral or tricuspid valve disease,<sup>72</sup> pulmonary hypertension, and right ventricular dysfunction.<sup>73</sup> The AHA/ACC guidelines do not advocate using dobutamine stress echocardiography with EF > 50%. Recent studies on the use of quantitative valve calcium scoring by MSCT may be useful.<sup>36-38</sup>

If both flow and gradient are used to subcategorize patients with severe AS, then four categories may be generated (Figure 3).<sup>58</sup> The four different hemodynamic categories of patients with AS on the basis of flow (normal, >200 mL/sec) and gradient (high, >40 mm Hg): normal flow and high gradient, normal flow and low gradient, low flow and high gradient, and low flow and low gradient.<sup>74</sup> The normal-flow, low-gradient entity is more difficult to explain, but this may be related to the use of stroke volume to define “normal flow” (i.e., stroke volume index  $\geq 35\text{ mL}/\text{m}^2$ ). Flow (in milliliters per second) is calculated as stroke volume divided by ejection time. It is possible that patients with normal flow and low gradient have normal stroke volume in the setting of a prolonged ejection time, thus resulting in a low gradient.

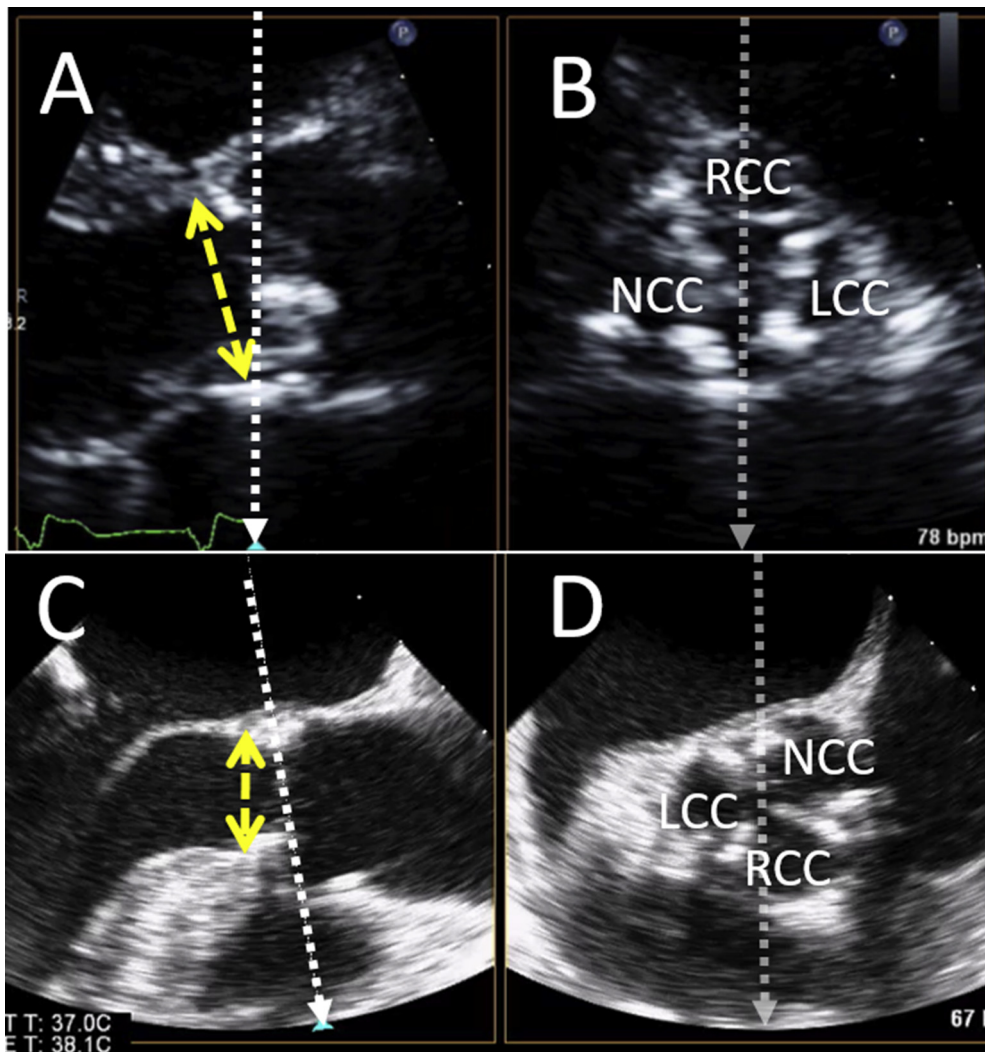
### Planimetry

Two-dimensional (2D) and 3D echocardiographic direct planimetry of the stenotic valve orifice can be also used to determine stenosis severity.<sup>48,75-78</sup> Using 2D transthoracic echocardiographic planimetric AVA, Okura *et al.*<sup>75</sup> showed that 2D transthoracic echocardiographic planimetry of AVA had a low standard error of estimates compared with valve area measured using transesophageal

**Table 1** Standard echocardiographic parameters used to assess the severity of AS

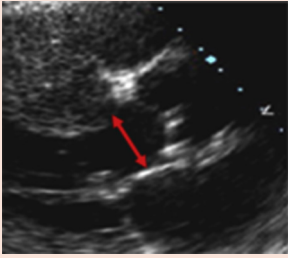
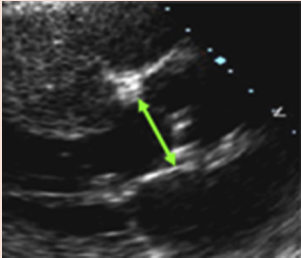
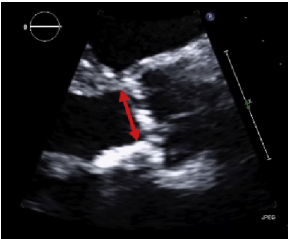
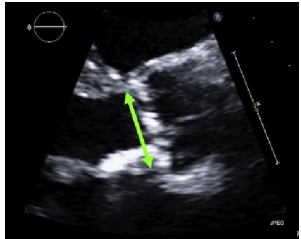
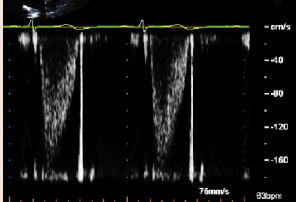
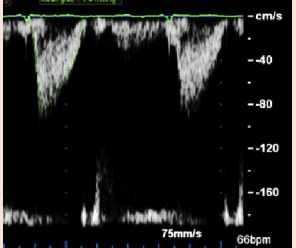
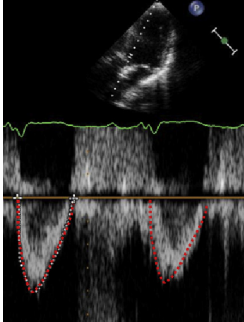
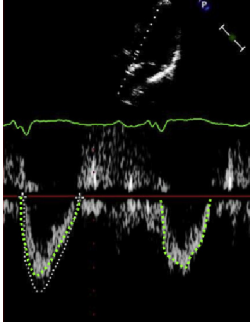
	Mild	Moderate	Severe
Valve anatomy	<ul style="list-style-type: none"> <li>Mild leaflet calcification or thickening with reduction in systolic motion</li> </ul>	<ul style="list-style-type: none"> <li>Mild to moderate leaflet calcification of a bicuspid or trileaflet valve with some reduction in systolic motion or</li> <li>Rheumatic valve changes with commissural fusion</li> </ul>	<ul style="list-style-type: none"> <li>Severe leaflet calcification or congenital stenosis with severely reduced leaflet opening</li> </ul>
Quantitative parameters (flow dependent)			
Peak velocity (m/sec)	2.0–2.9	3–3.9	$\geq 4$
Mean gradient (mm Hg)	<20	20–39	$\geq 40$
Quantitative parameters (flow independent)			
Doppler index	>0.5	0.26–0.5	$\leq 0.25$
AVA ( $\text{cm}^2$ )	>1.5	1.1–1.5	$\leq 1.0$
AVA index ( $\text{cm}^2/\text{m}^2$ )*	>0.85	0.61–0.85	$\leq 0.6$

\*Indexing valve area is particularly important in smaller patients with height < 135 cm (65 in), BSA < 1.5  $\text{m}^2$ , or body mass index < 22  $\text{kg}/\text{m}^2$ .



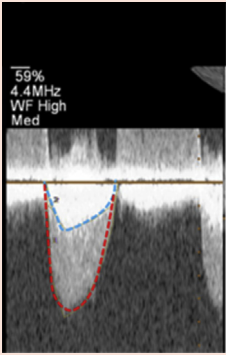
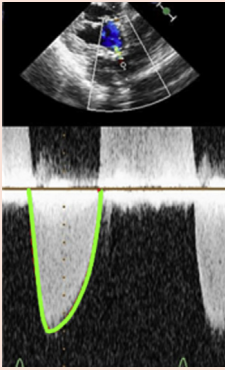
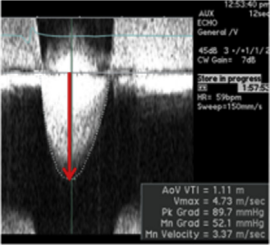
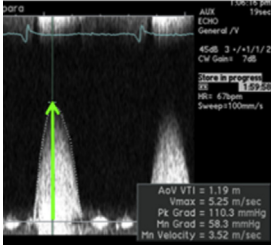
**Figure 2** Transthoracic and transesophageal echocardiographic optimization of LVOT measurement. Simultaneous biplane imaging from transthoracic (**A,B**) as well as transesophageal (**C,D**) imaging shows that an appropriately centered aortic valve in the long-axis view (**A** or **C**) will image the right coronary cusp (RCC) hinge point anteriorly (**B** or **D**) and the interleaflet trigone (between the left coronary cusp [LCC] and noncoronary cusp [NCC]) posteriorly. The maximum sagittal plane LVOT diameter (*yellow arrow*) should be measured from the inner edge to inner edge of the RCC hinge point/septal border to the posterior trigone/anterior mitral leaflet border. Importantly, the LVOT diameter measurement should avoid including ectopic calcium on the anterior mitral valve leaflet.

**Table 2** Summary of measurement pitfalls and recommended techniques for accurate quantitation of AVA

Pitfall	Incorrect example	Correct measurement	Correct example
Particularly in the setting of upper septal hypertrophy, there is progressive narrowing of the LVOT within the left ventricle; measuring the LVOT diameter 5–10 mm below the annulus will result in significant underestimation of the AVA by continuity equation (CE)		Measure the LVOT diameter at the level of the aortic annulus	
Ectopic calcium frequently is seen within the LVOT, on the LV side of the A2 mitral valve scallop is not circumferential, thus measuring inside this calcium ridge will result in significant underestimation of the AVA by CE		Exclude ectopic calcification in the LVOT or annulus when measuring the annulus	
Flow acceleration is seen proximal to a region of stenosis; placing the pulsed-wave sample volume at the annulus ( <i>red</i> ) will result in overestimation of the AVA by CE	At level of <i>red sample volume</i> 	Position the pulsed-wave sample volume in a region just proximal to the flow acceleration such that the spectral Doppler profile shows no opening or closure clicks	At level of <i>green sample volume</i> 
The appropriate pulsed-wave spectral profile should represent laminar flow (no spectral broadening) and trace the modal velocity (most frequently sampled velocity in the spectral profile, not the maximum velocity of a few red blood cells); tracing the faint spectral will overestimate stroke volume and AVA		Reducing the gain or increasing the reject will result in a spectral profile showing the modal velocity; the black-white interface should then be traced	

(Continued)

Table 2 (Continued)

Pitfall	Incorrect example	Correct measurement	Correct example
Off-axis imaging of the vena contracta (narrowest, highest velocity portion of the jet) will lead to underestimation of the severity of stenosis; seeing a “double envelope” of dense LVOT flow (blue trace), and fainter transaortic flow (red trace) may indicate that the insonation beam is angled away from the vena contracta		Adjust the imaging window to find the densest, most uniform continuous-wave spectral profile	
The direction of the transaortic jet may often be anterior and to the right; assuming the peak velocity from a single apical window will underestimate the severity of stenosis in up to 50% of patients		The right parasternal window in this patient showed peak velocities that were 0.5 m/sec higher; a multiwindow approach is always recommended	

echocardiographic planimetry, the continuity equation, or the Gorlin equation (0.04, 0.09, and 0.10 cm<sup>2</sup>, respectively). Importantly, planimetry and the Gorlin equation both measure the anatomic AVA, as the latter uses a correction coefficient for flow contraction.<sup>79</sup> This flow contraction leads to the formation of the “vena contracta” beyond the anatomic orifice area. The area of the vena contracta represents the effective orifice area calculated by the continuity equation and is theoretically different from the area measured by planimetry. Multiple studies have suggested that 3D planimetry AVA may be more accurate, allowing alignment of the tips of all leaflets in the short-axis view. These measurements may be larger than 2D measurements<sup>77,80</sup> and show a lower mean difference with continuity equation calculations.<sup>77</sup>

### Other Measures of AS Severity

Although measures of valve resistance, pressure recovery, energy loss, and arterial compliance and impedance are not recommended for routine clinical use, some may have significant prognostic information in certain subgroups of patients.

Differences in catheterization and echocardiographically measured gradients can arise in the setting of downstream pressure recovery.<sup>81-83</sup> This net pressure drop between the left ventricle and the ascending aorta is the pathophysiologically relevant measurement and more representative of the geometric valve area. The energy loss index (ELI) is another measure that attempts to account for the total fluid mechanical energy loss related to both valve area and ascending aortic area.<sup>84</sup> The ELI is calculated as  $ELI = [effective\ orifice\ area \times A_A/A_A - effective\ orifice\ area]/BSA$ . Similar to valve area, it is less flow dependent than gradient

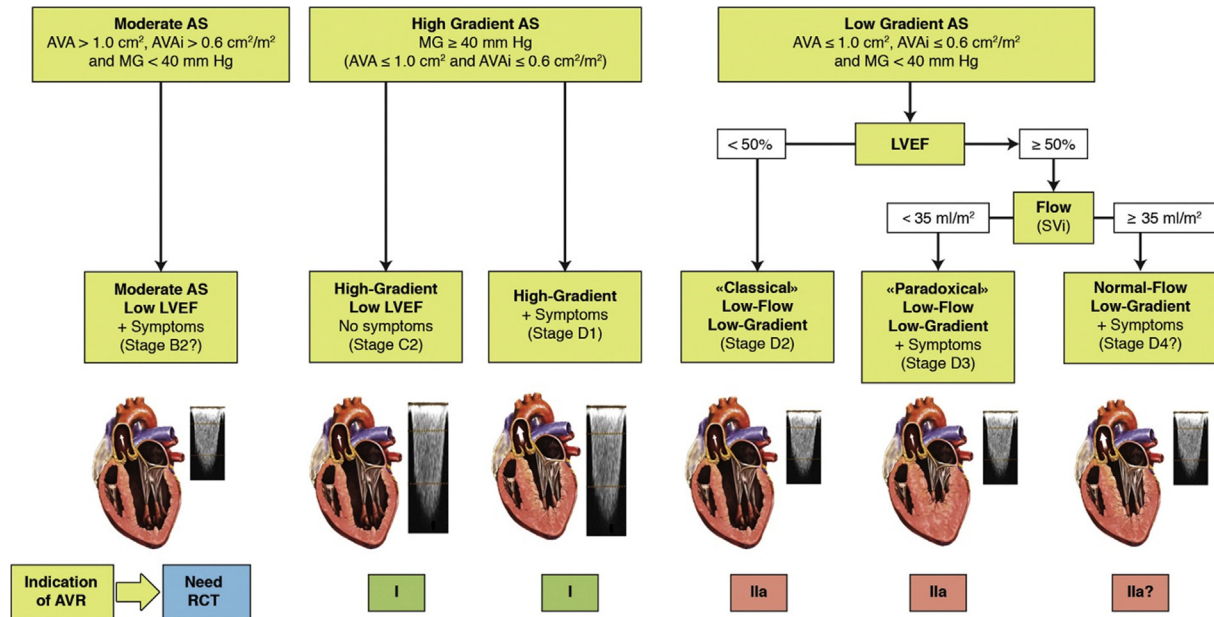
or peak velocity, takes into account pressure recovery, and is roughly equivalent to effective orifice area measured by catheterization.<sup>85</sup> Using the ELI, a substudy of the Simvastatin and Ezetimibe in Aortic Stenosis trial reclassified 47.5% of patients from severe to nonsevere AS.<sup>86</sup> The energy loss is most significant in small aortas (<30 mm). An ELI of  $\leq 0.5$  to 0.6 cm<sup>2</sup>/m<sup>2</sup> is consistent with severe AS.<sup>86,87</sup>

Finally, an index of global LV hemodynamic load, valvuloarterial impedance ( $Z_{va}$ ), accounts for both the load of the aortic valve and the increase in vascular resistance. An increase in systemic vascular resistance may be a compensatory mechanism in the setting of reduced transvalvular flow. Concomitant arterial hypertension is found to be present in a large proportion (35%–51%) of patients with AS.<sup>88-90</sup>  $Z_{va}$  is calculated as  $Z_{va} = \text{systolic blood pressure} + \Delta P_{\text{mean}}/\text{stroke volume index}$ .<sup>88</sup> Several investigators have shown that the risk for mortality was increased with an increase in  $Z_{va}$ .<sup>88,89,91-93</sup> Hachicha *et al.*<sup>89</sup> found an increase in mortality of 2.76-fold in patients with  $Z_{va} \geq 4.5$  mm Hg · mL<sup>-1</sup> · m<sup>2</sup> and by 2.30-fold in those with  $Z_{va}$  between 3.5 and 4.5 mm Hg · mL<sup>-1</sup> · m<sup>2</sup> after adjusting for other risk factors.

### Stress Testing in AS

The indications for stress testing for severe AS include determination of the etiology of symptoms in the setting of nonsevere disease, confirmation of asymptomatic status in the setting of severe disease, and evaluation of patients with concomitant valvular and myocardial dysfunction.<sup>94</sup>

Because of the poor prognosis associated with symptom onset,<sup>95</sup> determination of symptom status is an important role for stress testing in patients reporting no symptoms with severe AS.<sup>22,96</sup> A number of



**Figure 3** Classification and characterization of the different types of AS according to AVA, gradient, LVEF, and flow. Classification of types of AS, including only the categories associated with symptoms and/or depressed LVEF. It does not include stage C1 (i.e., patients with high-gradient AS, no symptoms, and preserved LVEF). *Question mark* indicates stage labels or indications for aortic valve replacement (AVR) that are proposed but are not included in the guidelines and will need to be further tested and validated. AVAi, Indexed AVA; MG, mean gradient; RCT, randomized controlled trial; SVI, stroke volume index. Reproduced with permission from Clavel et al.<sup>58</sup>

parameters have been used to indicate a positive exercise treadmill test in the setting of AS:

- development of symptoms (limiting breathlessness, chest pain or tightness, dizziness, and syncope);<sup>97,98</sup>
- development of arrhythmias (three consecutive ventricular premature beats or other complex ventricular arrhythmias);<sup>97,98</sup>
- blood pressure failing to increase by 20 mm Hg<sup>97,99</sup> or a decrease in blood pressure of ≥10 mm Hg;<sup>98</sup> and
- development of horizontal or down-sloping ST-segment depression (≥1 mm in men, ≥2 mm in women)<sup>97</sup> or ST-segment depression ≥ 5 mm measured 80 msec after the J point.<sup>98</sup>

For patients with negative stress test results, outcomes may still not be benign, with the associated risk for symptom onset as well as sudden death.<sup>5,100</sup> In patients with moderate or severe AS, an increase in mean gradient of ≥18 to 20 mm Hg during exercise testing predicts a higher risk for progression to symptoms and adverse events.<sup>98,99</sup> To test the hypothesis that TAVR in asymptomatic patients may improve long-term outcomes compared with watchful waiting, the Early-TAVR clinical trial ([ClinicalTrials.gov](https://clinicaltrials.gov/ct2/show/study/NCT03042104) identifier NCT03042104) is currently enrolling.

### Detection of Associated Ventricular and Valvular Abnormalities

An essential part of the evaluation of every patient with AS is the assessment of chamber sizes, ventricular function, and concomitant valvular disease.

In chronic AS, changes in LV geometry are both adaptive and pathologic. As the pressure overload increases, an increase in wall thickness maintains normal wall stress and EF. Both an increase in wall thickness with normal LV mass (concentric remodeling) and increased LV mass (concentric hypertrophy) are frequently seen. Increased wall

thickness in AS has been associated with impaired calcium handling, cytoskeletal changes, apoptosis, and increased collagen fiber deposition. These changes result in detectable reduced deformation characteristics and chamber compliance, before any change in EF. This cascade of events eventually leads to decreased stroke volume and increased filling pressure, resulting in heart failure with preserved EF. Thus strain imaging as well as diastolic function parameters may be early markers of abnormal LV function. Importantly, the European Association of Cardiovascular Imaging and American Society of Echocardiography consensus on the standardization of strain imaging defines deformation imaging terminology, the type of stored data that are used for quantitative analysis, the modality of measuring basic parameters, the definitions of parameters, and the results output with the aim of reducing intervendor variability.<sup>101</sup>

**Ejection Fraction.** Long-standing severe pressure overload, particularly in the setting of concomitant hypertension,<sup>13,102</sup> often leads to reduced LVEF and cardiac output. Numerous studies have documented an increase in mortality associated with reduced EF, as well as poor renal function in the setting of severe, symptomatic AS irrespective of an intervention on the aortic valve.<sup>103,104</sup> A recent meta-analysis of 26 studies and nearly 6,900 patients showed that patients with baseline low EF and severe AS have higher mortality following TAVR compared with those with normal EF, despite a significant and sustained improvement in LV function.<sup>105</sup>

**Strain Imaging.** In the presence of normal EF, increasing severity of AS was associated with reduced global longitudinal strain (GLS).<sup>106,107</sup> GLS was found to be a predictor of all-cause mortality,<sup>108,109</sup> and GLS was a superior predictor of outcomes in patients referred for surgery compared with standard predictors such as risk score, presence of ischemic heart disease, and EF.<sup>110</sup> In patients with low flow, low gradient, and preserved EF, GLS was independently

associated with survival after aortic valve replacement.<sup>111</sup> In patients with low flow, low gradient, and reduced EF, stress GLS measured during dobutamine stress echocardiography may provide incremental prognostic value beyond GLS measured at rest.<sup>112</sup> Three-dimensional GLS may be a better predictor of outcome compared with 2D strain.<sup>113</sup> In patients with moderate or severe AS and concomitant coronary disease, worse apical and mid longitudinal strain parameters were predictive of significant coronary stenosis.<sup>114</sup>

Strain may become a useful predictor of preclinical disease severity. Recent studies have suggested that conservative management of patients with severe but asymptomatic AS may result in poor outcomes.<sup>100</sup> In a propensity-matched, prospective study, Taniguchi *et al.*<sup>100</sup> showed that the cumulative 5-year incidence of all-cause death and heart failure hospitalization was significantly lower in the initial valve replacement group than in the conservative group (15.4% vs 26.4% [ $P = .009$ ] and 3.8% vs 19.9% [ $P < .001$ ], respectively). Because mortality is significantly associated with symptom development,<sup>95</sup> strain has been postulated as a possible early marker of ventricular dysfunction in asymptomatic patients with severe AS and thus may be a useful tool in determining the timing of intervention in this population. Carasso *et al.*<sup>115</sup> showed that longitudinal strain was low in asymptomatic patients with severe AS with supernormal apical circumferential strain and rotation. In symptomatic patients, however, longitudinal strain was significantly lower, with no compensatory circumferential myocardial mechanics. Other investigators have suggested that after adjusting for AS severity and EF, only basal longitudinal strain (and not GLS) was an independent predictor of symptomatic status.<sup>116,117</sup> In fact, following TAVR, the improvement in GLS may be a result of basal and mid segment improvement only.<sup>118</sup>

**Diastolic Function.** The effect of LV diastolic function on outcome in AS is controversial. Biner *et al.*<sup>119</sup> showed that in patients with symptomatic severe AS with LV systolic dysfunction (LVEF  $\leq 50\%$ ) or asymptomatic severe AS with preserved LV systolic function (LVEF  $> 50\%$ ), there was significantly higher 1-year survival rate in patients with E/e' ratios  $< 15$  compared with those with E/e' ratios  $\geq 15$  among both asymptomatic and symptomatic patients. Higher in-hospital mortality or major morbidity may also be associated with an elevated E/e' ratio.<sup>120</sup> Other studies have shown marked improvements in diastolic function parameters following intervention<sup>121</sup> but failed to show an association between baseline diastolic function and outcomes.<sup>122</sup>

**Concomitant Valve Disease.** Additional valve disease may also affect outcomes following TAVR. Studies from the surgical literature have been conflicting with regard to treatment of coexistent significant mitral regurgitation (MR) and AS.<sup>123,124</sup> Barbanti *et al.*<sup>125</sup> found moderate or severe mitral MR in about 20% of patients in the Placement of Aortic Transcatheter Valves (PARTNER) IA cohort at baseline. MR improved in 69.4% of surgical aortic valve replacement patients and 57.7% of TAVR patients.<sup>125</sup> It was uncommon to see worsening of MR following intervention. An increase in mortality at 2 years with moderate or severe MR was seen only in the surgical aortic valve replacement cohort (49.8% vs 28.1%; adjusted hazard ratio [HRI], 1.73; 95% CI, 1.01–2.96;  $P = .04$ ), with no adverse outcomes seen in the TAVR cohort. Persistent moderate or severe MR did not affect LV remodeling.

Significant tricuspid regurgitation (TR) may also affect outcomes. Of the patients in the PARTNER IIB cohort, 26.6% had moderate or severe TR at baseline. Compared with patients with less than moderate TR, these patients had lower LVEF and stroke volume index, larger left atrial size, and greater prevalence of moderate or

severe MR. In addition, these patients had larger right atria and ventricles, with worse right ventricular function and higher right ventricular systolic pressure estimates. More severe TR was associated with increased 1-year mortality ( $P < .001$ ), as were right atrial and right ventricular enlargement and right ventricular dysfunction ( $P > .001$ ). At 30 days, about 30% of patients with baseline moderate or severe TR improved to less than moderate TR, and this improvement was associated with improved survival at 1 year. In patients with concomitant moderate or severe MR, moderate or severe TR was not associated with increased hazard of death compared with less than moderate TR. In patients with minimal MR, multivariate adjustment continued to show that severe TR was associated with increased mortality (HR, 3.20; 95% CI, 1.50–6.82;  $P = .003$ ) along with right atrial and right ventricular enlargement ( $P < .001$ ).

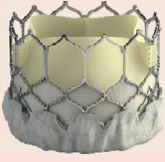

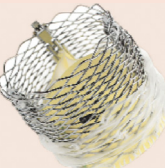


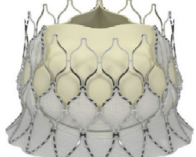
## IMAGING FOR TAVR

An effective imager on the heart team must understand the anatomy relevant to the device and the procedural steps for device implantation, because at each stage of the procedure there are different roles for imaging. Table 3 shows some of the commercially available as well as investigational THV devices with important valve composition and considerations. Multimodality imaging used in a TAVR program involves the use of MSCT, cardiac magnetic resonance imaging, fluoroscopy, and echocardiography, with the ultimate goals of appropriate patient selection, procedural guidance, and detection of complications. Although MSCT has become a standard preprocedural imaging modality for measurement of the aortic annular area and perimeter,<sup>126,127</sup> vascular access, coronary artery position, calcium burden, and fluoroscopic projection angles,<sup>128</sup> the dynamics of the procedural environment are unique and require constant communication and adaptability, for which echocardiography is the optimal imaging modality. Intraprocedural echocardiographic findings must be interpreted in the context of patient's hemodynamics, influenced by the presence of anesthesia and by the procedure itself, and decisions must be made in real time, after careful consideration and deliberation of all aspects of risks and benefits. Intraprocedural transesophageal echocardiography (TEE), with the added value of real-time 3D imaging techniques, provides an undisputed wealth of continuous, physiologic information both in procedural planning and guidance and in detecting complications. In this section we highlight some of the unique benefits of intra-procedural TEE in patients undergoing TAVR.

### Predeployment Imaging

The comprehensive intraoperative preprocedural evaluation is summarized in Table 4. Preprocedural assessment of aortic root anatomy and dimensions is paramount to the selection of the appropriate prosthesis. Several factors are considered when selecting an optimal prosthetic valve for a patient: aortic annulus and geometry, aortic root and LVOT anatomy, angulation of the aorta (aortoventricular angle), coronary height, and amount and distribution of calcification.<sup>129</sup> Undersizing a prosthetic valve may lead to PAR or device embolization, while oversizing may result in aortic root rupture, coronary ostia occlusion, or conduction abnormalities. Evaluation of the aortic root starts with measurement of the aortic annulus. Various vendor-specific annular measurement packages measure maximum and minimum diameters, perimeter, and area of the aortic annulus. Although the word *annulus* implies a circular structure, there is no histologic or

**Table 3** Examples of THVs commercially available or in trials

Transcatheter valve name (manufacturer)	Example	Features	Procedural/imaging nuances
SAPIEN 3 (Edwards Lifesciences), commercially available		<ul style="list-style-type: none"> <li>• Cobalt chromium frame</li> <li>• Bovine pericardial leaflets</li> <li>• PET cuff</li> <li>• Balloon-expandable, typically deployed during rapid pacing</li> </ul>	<ul style="list-style-type: none"> <li>• Shortens from skirt end</li> <li>• Positioning by echocardiography ensures that the aortic end is below the sinotubular junction and covers the native leaflets</li> <li>• May be ideal for high risk for coronary obstruction and distorted aortic anatomy</li> <li>• May be appropriate for bicuspid aortic valve</li> </ul>
EvolutPro (Medtronic), commercially available		<ul style="list-style-type: none"> <li>• Supra-annular valve position</li> <li>• Porcine pericardial leaflets</li> <li>• External PET wrap</li> <li>• Self-expanding frame</li> <li>• Repositionable</li> <li>• Rapid pacing not required</li> </ul>	<ul style="list-style-type: none"> <li>• Ideal position of the ventricular end once deployed should be 2–4 mm below the native annulus (and not <math>\geq 6</math> mm)</li> <li>• May be more difficult to accurately position with a horizontal aorta or annular/STJ distortion</li> <li>• May be ideal for preexisting mitral bioprostheses</li> <li>• Has been used for primary AR</li> </ul>
Lotus Edge (Boston Scientific, Natick, MA), investigational device		<ul style="list-style-type: none"> <li>• Mechanical expansion of device</li> <li>• Repositionable before release</li> <li>• Adaptive Seal skirt</li> <li>• Rapid pacing not required</li> </ul>	<ul style="list-style-type: none"> <li>• Relies on fluoroscopic positioning with assistance from echocardiography for paravalvular leak assessment and need for repositioning</li> <li>• May be appropriate for bicuspid aortic valve</li> </ul>
ACURATE neo (Boston Scientific), investigational device		<ul style="list-style-type: none"> <li>• Supra-annular valve</li> <li>• Self-expanding</li> <li>• Partially recapturable</li> <li>• Three stabilizing arches</li> <li>• Rapid pacing not required</li> </ul>	<ul style="list-style-type: none"> <li>• Echocardiographic positioning of the ventricular end below the annulus</li> <li>• Has been used for primary AR</li> </ul>
JennaValve (JenaValve, Munich, Germany), investigational device		<ul style="list-style-type: none"> <li>• Feeler-guided anatomic positioning</li> <li>• JenaClip anchoring to native leaflets</li> <li>• Retrievable and repositionable</li> <li>• Rapid pacing not required</li> </ul>	<ul style="list-style-type: none"> <li>• Echocardiographic guidance of anatomic positioning to align clips and commissures</li> <li>• Treats primary AS and primary AR</li> </ul>
Centera (Edwards Lifesciences), investigational device		<ul style="list-style-type: none"> <li>• Self-expandable, nitinol stent with bovine pericardial tissue valve</li> <li>• Annular position</li> <li>• PET fabric</li> <li>• Motorized deployment</li> <li>• Repositionable and retrievable</li> </ul>	<ul style="list-style-type: none"> <li>• Echocardiography for paravalvular leak assessment and need for repositioning</li> </ul>

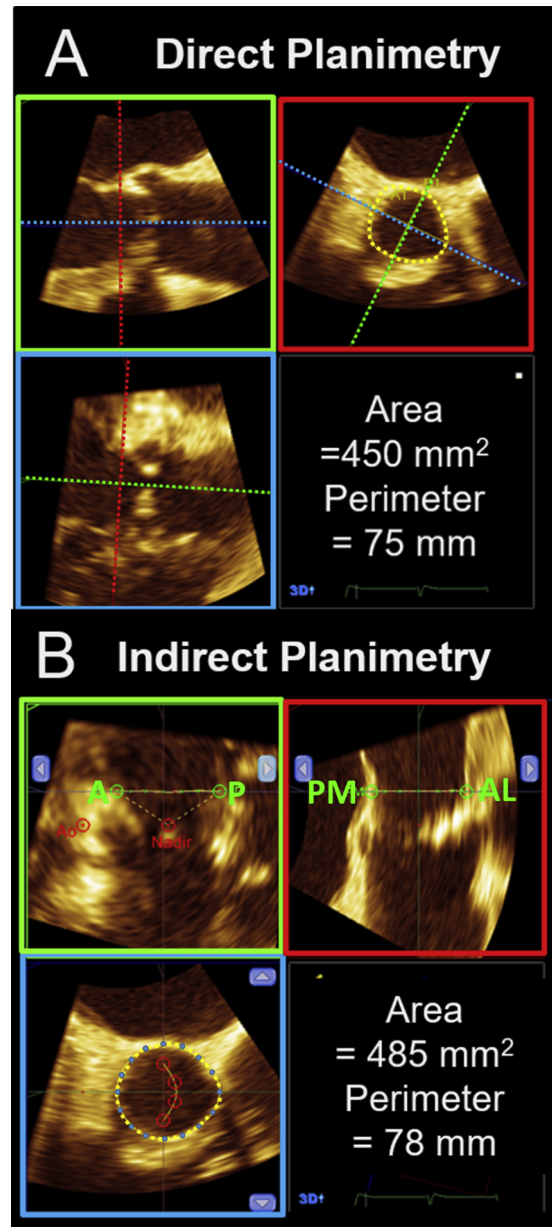
PET, Polyethylene terephthalate; STJ, sinotubular junction.

**Table 4** Preprocedural structural and functional assessment by echocardiography

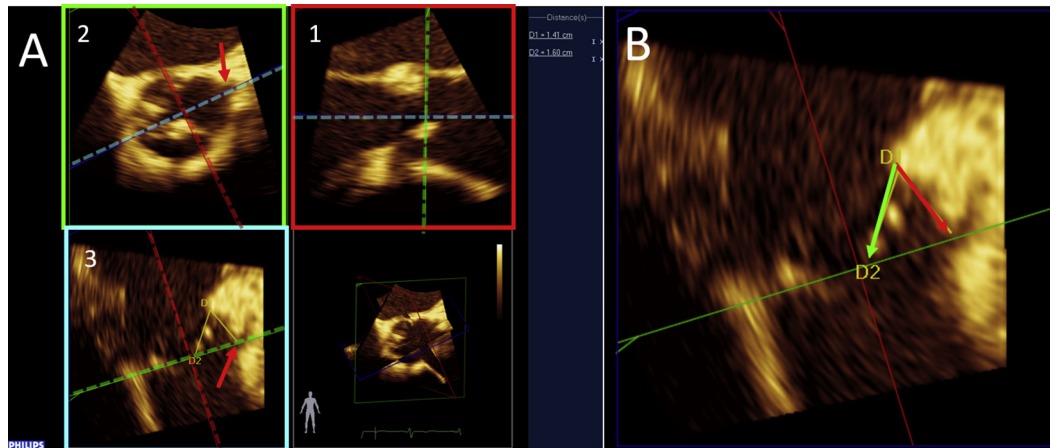
- Aortic valve and root
  - Aortic valve morphology
    - Confirm pathology
    - Assess presence of AR
    - Number of cusps (bicuspid/tricuspid)
    - Volume and distribution of calcifications
  - Aortoannular complex dimensions
    - Aortic annular dimensions (major, minor, and average diameters, perimeter, area)
    - Sinuses of Valsalva diameter
    - Sinotubular junction diameter
    - Aortic annulus to coronary artery ostia distances
  - Aortic valve hemodynamics
    - Aortic valve peak velocity, peak and mean gradients, and calculated valve area
    - Dimensionless index
    - Stroke volume and stroke volume index
  - LVOT
    - Extent and distribution of calcium
    - Presence of sigmoid septum and dynamic narrowing
- Mitral Valve
  - Severity and mechanism of MR
  - Presence of mitral stenosis
  - Severity of ectopic calcification of the anterior leaflet
- LV size and function
  - Exclude intracardiac thrombus
  - Wall motion assessment
  - EF
  - Stroke volume and cardiac output
- Right heart
  - Right ventricular size and function
  - Tricuspid valve morphology and function
  - Estimate of pulmonary artery pressures
- Presence of pericardial effusion

anatomic boundary to define it and to guide measurement. Rather, the measurements are performed in a virtual plane defined by the nadirs of the semilunar leaflet attachments. Traditionally, the aortic annulus has been described by a single measurement from 2D transthoracic echocardiography (TTE) or TEE. However, the three-dimensionality and the complexity of the aortic root anatomy can be adequately appreciated only by using a 3D imaging modality. This has been investigated in studies that showed that the incidence of more than mild PAR was significantly lower when sizing of the aortic annulus was performed using MSCT compared with sizing performed by 2D echocardiography.<sup>130,131</sup> Two-dimensional echocardiography consistently underestimates the size of the aortic annulus for several reasons: (1) a linear dimension assumes a circular geometry of the annulus, while a growing body of literature has shown that it is nearly uniformly oval shaped<sup>132,133</sup>; (2) the long-axis or sagittal plane in which the measurement is performed may not bisect the maximum dimension of the annulus (i.e., imaging of the hinge point to hinge point rather than hinge point to fibrous trigone); and (3) the measurement in the long-axis view generally represents the smaller diameter of the noncircular annulus.

Three-dimensional echocardiography overcomes the limitations of 2D imaging by allowing measurements of the annular area and perimeter. Although 3D TTE lacks the spatial resolution for adequate measurements of the aortic root, several recent studies have shown that



**Figure 4** Multiplanar reconstruction of a 3D data set by two methods. **(A)** Multiplanar reconstruction of the virtual annular plane (red box) obtained by aligning the long-axis transverse plane (green box) and coronal plane (blue box). The annulus is measured by direct planimetry. **(B)** Indirect planimetry method, which uses a mitral valve software package, QLAB MVQ software (Philips Medical Systems, Andover, MA), thus tricking the system into measuring the aortic annulus as if it were a mitral annulus. The top two quadrants of **(B)** show the positioning of the “anterior” (A), “posterior” (P), “postero-medial” (PM), and “anterolateral” (AL) annular indicators. On successive rotations of the two orthogonal long-axis planes (green and red boxes), the annular plane is identified and automatically shown in the annular short axis of the blue plane (blue dots). The complete the annular plane is created without actually planimetry on the annular short axis and is thus an “indirect” planimetric method. Both methods yield the annular area, perimeter, and maximum and minimum dimensions of the annulus.



**Figure 5** Left coronary artery height measured by multiplanar reconstruction. Because the left coronary artery lies in the coronal plane, imaging of the height of the left main coronary artery requires 3D imaging and reconstruction. In the multiplanar reconstruction (**A**), the *blue plane* is first aligned along the long axis of the aorta from the sagittal (*red*) plane. Second, the *blue plane* is aligned in the transverse (*green*) plane with the left coronary artery (*red arrow*). The coronal (*blue*) plane is now the plane of the left coronary artery (*red arrow*). This *blue plane* (**B**) is then used to measure the distance from the hinge point of the left coronary cusp to the left coronary orifice (*red arrow*) as well as the length of the left coronary cusp (*green arrow*).

**Table 5** Intraprocedural structural and functional TEE

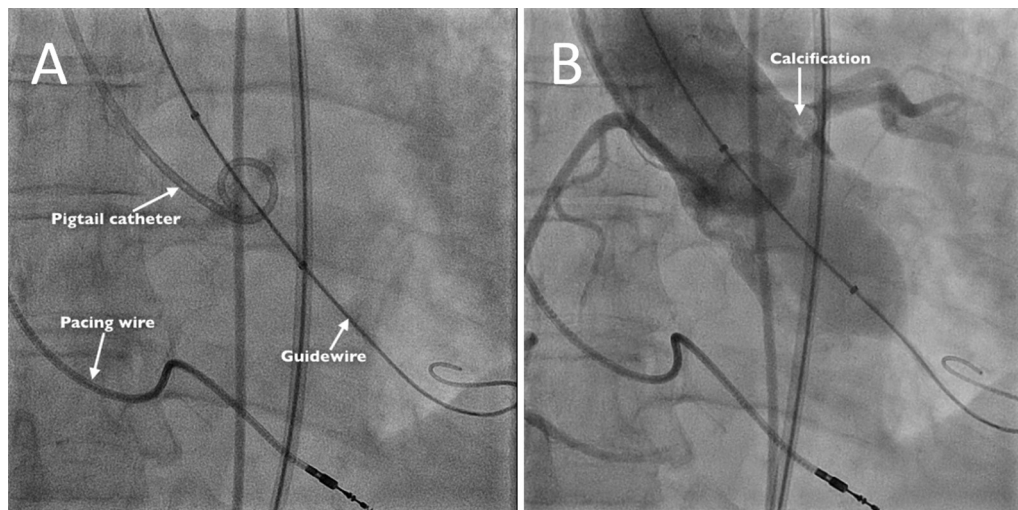
<ul style="list-style-type: none"> <li>Positioning of wires (pacer, pigtail and guidewire)</li> </ul>	<ul style="list-style-type: none"> <li>May facilitate crossing the aortic valve</li> <li>Identify entrapment in the mitral valve apparatus</li> <li>Exclude presence of new/worsened pericardial effusion</li> <li>Identify thrombus on wires or catheters</li> </ul>
<ul style="list-style-type: none"> <li>Balloon aortic valvuloplasty</li> </ul>	<ul style="list-style-type: none"> <li>Evaluate relationship of leaflet calcification with the aortic root walls</li> <li>Exclude presence of new/worsened pericardial effusion</li> <li>Exclude presence of new/worsened MR</li> <li>Evaluate mobility of aortic valve cusps and severity of AR</li> <li>Exclude new wall motion abnormalities, or confirm flow by color flow Doppler in the coronary arteries</li> </ul>
<ul style="list-style-type: none"> <li>Positioning and deployment of transcatheter valve</li> </ul>	<ul style="list-style-type: none"> <li>Balloon-expandable valve                             <ul style="list-style-type: none"> <li>Confirm the aortic end position of the balloon-expandable transcatheter valve below STJ and covering leaflets</li> <li>Watch displacement of calcium for risk for rupture or coronary occlusion during controlled balloon inflation</li> </ul> </li> <li>Self-expanding valve                             <ul style="list-style-type: none"> <li>Confirm the ventricular end position of the self-expanding transcatheter valve 2–4 mm below the annular plane</li> <li>Confirm final position once released</li> </ul> </li> </ul>
<ul style="list-style-type: none"> <li>Transapical cannulation</li> </ul>	<ul style="list-style-type: none"> <li>Confirm site of transapical puncture (away from the interventricular septum and right ventricle)</li> <li>Evaluate retrograde position of the guidewire through the aortic valve</li> <li>Exclude entrapment in the mitral valve apparatus and worsened MR</li> </ul>
<ul style="list-style-type: none"> <li>Post-deployment assessment</li> </ul>	<ul style="list-style-type: none"> <li>Assess the transcatheter valve                             <ul style="list-style-type: none"> <li>Position, shape, peak/mean gradient, and AVA</li> </ul> </li> <li>Presence of central or paravalvular regurgitation</li> <li>Patency of coronary arteries</li> <li>Presence of pericardial effusion or focal rupture</li> <li>Assess ventricular and other valvular function</li> </ul>

STJ, Sinotubular junction.

measurements performed by multiplanar reconstruction of 3D transthoracic echocardiographic data sets yields comparable results with those obtained using MSCT, at the same time avoiding the risks associated with exposure to radiation and contrast dye.<sup>50,134,135</sup> Multiplanar reconstruction of a 3D data set facilitates direct measurements of the major and minor diameters, as well as annular area and perimeter from an on-axis short-axis plane (Figure 4A).

Other investigators have used vendor-specific software originally designed for the mitral valve to indirectly planimeter the annulus<sup>136</sup> (Figure 4B) and proved that annular measurements by both 3D TEE and MSCT predicted mild or greater PAR with equivalent accuracy.<sup>51</sup>

Besides dimensions of the aortic annulus, other measurements of the aortoannular complex should be performed, such as the size of the sinuses of Valsalva, diameter of the aorta at the sinotubular



**Figure 6** Fluoroscopic imaging during TAVR. **(A)** Fluoroscopic image of the wires shows the relative positions of the pigtail catheter in the right coronary sinus of Valsalva, as well as the pacing wire in the right ventricle and guidewire in the left ventricle. **(B)** Fluoroscopic image during maximal balloon inflation. In this image of maximal balloon inflation, the calcific left coronary cusp can be imaged occluding the left main coronary artery. In addition, contrast injection reveals significant leak around the undersized balloon, indicating a risk for paravalvular regurgitation.

junction, and the distance of the coronary artery ostia from the annulus.<sup>129</sup> Because the left coronary artery ostium lies in the coronal plane, the coronary height can be measured only by multiplanar reconstruction (Figure 5). Data from a large multicenter registry of coronary obstruction after TAVR, showed the left coronary artery was most commonly involved (88.6%), with lower mean left coronary artery ostia height ( $10.6 \pm 2.1$  vs  $13.4 \pm 2.1$  mm,  $P < .001$ ) and sinus of Valsalva diameter ( $28.1 \pm 3.8$  vs  $31.9 \pm 4.1$  mm,  $P < .001$ ) compared with control subjects.<sup>9</sup> The distribution of calcium in the aortic root, extension into the LVOT and aortomitral curtain, and proximity of calcium to the coronary artery ostia should also be described. LVOT morphology with the presence of basal septal hypertrophy as well as the presence of midventricular hypertrophy is important to assess, as the development of subvalvular dynamic obstruction with hemodynamic instability after valve deployment has been described.<sup>137</sup>

### Intraprocedural Imaging

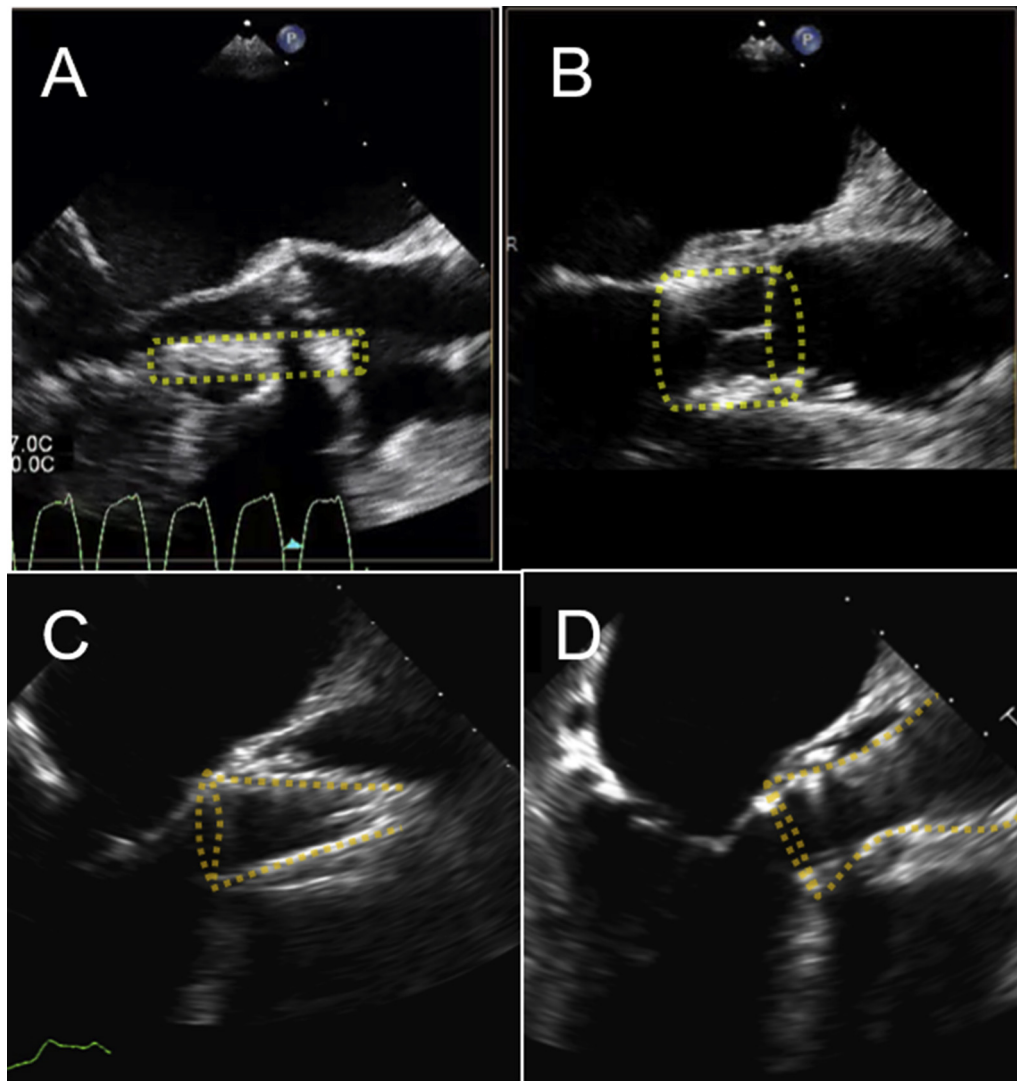
Procedural guidance can be ensured through a combination of imaging modalities such as fluoroscopy, aortography, and echocardiography. The significant advantage of TEE is continuous monitoring of all aspects of the procedure. In situations of acute hemodynamic changes, TEE can readily diagnose complications associated with transvalvular wire or delivery system or balloon valvuloplasty. Table 5 summarizes intraprocedural imaging with TEE.

Several wire positions are typically confirmed by fluoroscopy (Figure 6A) but may also be imaged by echocardiography. These include the pacing wire in the right ventricular apex, the transvalvular stiff guidewire within the left ventricle, and the pigtail catheter placed in the sinuses of Valsalva at the level of the noncoronary cusp (for self-expanding valves) and right coronary cusp (for balloon-expandable valves). Placement of wires can lead to thrombus formation, ventricular perforation, and accumulation of pericardial effusion as well as disruption of mitral valve apparatus with worsening MR.

Before positioning of the valve, predilation of the aortic valve may be performed with balloon aortic valvuloplasty and rapid ventricular

pacing during inflation. Besides facilitating subsequent transvalvular positioning of the delivery system, radiographic contrast opacification of the root during balloon aortic valvuloplasty provides useful information regarding possible coronary ostia occlusion by native leaflets or calcifications and appropriate sizing of the valve by visualization of the leak around the maximally inflated balloon (Figure 6B). Although hemodynamic instability may occur because of rapid ventricular pacing, other causes of hemodynamic instability should be ruled out after balloon deflation: pericardial effusion and tamponade due to aortic root rupture, severe left or right ventricular dysfunction due to acute coronary occlusion, or severe acute aortic regurgitation (AR).<sup>24</sup>

It is imperative that the transcatheter valve be positioned precisely according to vendor-specific recommendations. High implantation (too aortic relative to the annulus) may result in transcatheter valve embolization into the aorta, aortic intima injury, AR, or coronary artery ostia obstruction. Low implantation (too ventricular relative to the annulus) may result in disturbance of the mitral valve apparatus and MR, impingement on the atrioventricular node and conduction abnormalities, or transcatheter valve embolization into the ventricle. Although the landing zone is standardized and depends on the type of the valve (Table 3), each case is individualized on the basis of the size of the transcatheter valve, anatomy of the aortic root and LVOT, and position of the left coronary artery. Although fluoroscopy plays a pivotal role in positioning the transcatheter valve, TEE can provide complementary information. For the third-generation balloon-expandable SAPIEN 3 (Edwards Lifesciences, Irvine, CA), the final implantation depth should be 1 to 2 mm below the native aortic annulus.<sup>24</sup> Because the design of the valve allows shortening after deployment only from the ventricular side, the positioning of the valve before deployment should focus on the aortic edge, which should be covering the native leaflets and remain below the sinotubular junction<sup>24</sup> (Figures 7A and 7B). For the second-generation self-expandable valve CoreValve Evolut R (Medtronic, Minneapolis, MN), an optimal implantation depth is 2 to 4 mm below the aortic annulus.<sup>129</sup> The deployment of the self-expandable valve occurs in a controlled manner, over several minutes. Because of the initial



**Figure 7** Predeployment and final position of the transcatheter aortic valve. **(A)** Balloon-expandable valve position before deployment. The aortic edge is below the sinotubular junction and covering the leaflets. After deployment **(B)**, the ventricular edge should be 1 to 2 mm below the annulus, but the final position may depend on the degree of oversizing. **(C)** Position of the self-expanding valve before deployment. The ventricular edges are typically not symmetrically below the annulus (lower anteriorly) but should be 3 to 5 mm below the annular plane. Following release of the aortic tabs **(D)**, the valve typically pivots, and the anterior edge moves superiorly and the valve aligns coaxial with the long axis of the aorta.

posterolateral orientation of the valve during deployment, the posterior edge of the valve is initially higher (more aortic) than the anterior edge (Figure 7C). After full release from the delivery system, the valve pivots, the anterior edge moves superiorly, and the valve aligns coaxial with the long axis of the aorta<sup>24</sup> (Figure 7D).

### Postprocedural Imaging

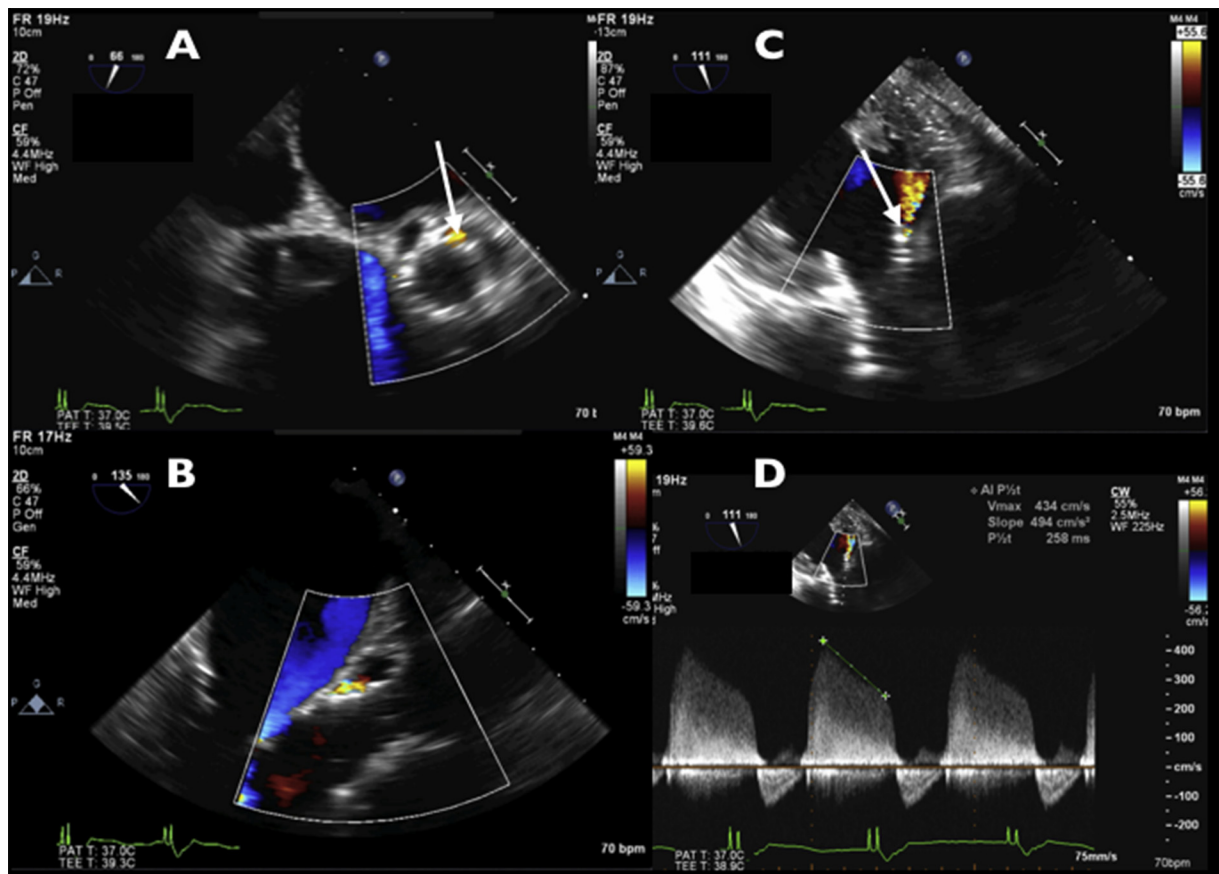
An assessment of the position of prosthesis, leaflet mobility, and the shape of the deployed valve should be performed immediately following TAVR.<sup>24</sup> Complications such as coronary occlusion or aortic rupture are typically accompanied by significant hemodynamic compromise. The most common complication following TAVR is PAR, with greater than mild regurgitation seen in 0% to 24% of patients in early experience<sup>12,132,138-147</sup> and only 0% to 6% with current valve iterations.<sup>2,148-150</sup> Rapid assessment of PAR following TAVR is essential because this post-TAVR complication can be treated

intraoperatively with balloon dilatation, valve-in-valve salvage, or paravalvular device implantation.<sup>151,152</sup> PAR assessment is particularly important following deployment of a repositionable transcatheter valve, but cine angiography and invasive hemodynamics may be challenging because of the atypical characteristics of the regurgitation jets (Table 6).

Echocardiography, either transthoracic or transesophageal, remains the preferred method for assessing PAR for a number of reasons. Echocardiography can identify the location, number, and extent of the regurgitation jets and discriminate between transvalvular (central) and PAR (Figure 8). Importantly, echocardiography can determine the etiology of PAR: suboptimal valve position, valve under- or overexpansion or asymmetry, or ectopic annular or subannular calcification. The assessment of location and etiology will determine the appropriate intraoperative management of this complication: valve-in-valve for central AR and postdilatation, PAR closure with a leak device, or valve-in-valve. It is important to scan

**Table 6** Limitations of other intraprocedural imaging modalities for assessing PAR

Cine angiography	Hemodynamic parameters
Dependent on <ul style="list-style-type: none"> <li>• Observer's experience</li> <li>• Intensity of fluoroscopy</li> <li>• Volume of contrast injected</li> <li>• Type and position of catheter tip<sup>140</sup></li> </ul> Inability to differentiate intra- from paravalvular regurgitation Exposure to radiation Exposure to angiographic contrast Limited accuracy and reproducibility <sup>153</sup>	Inability to differentiate intra- from paravalvular regurgitation Influenced by abnormal ventricular and aortic compliance Dependent on heart rate Significant overlap between grades of regurgitation <sup>140</sup>

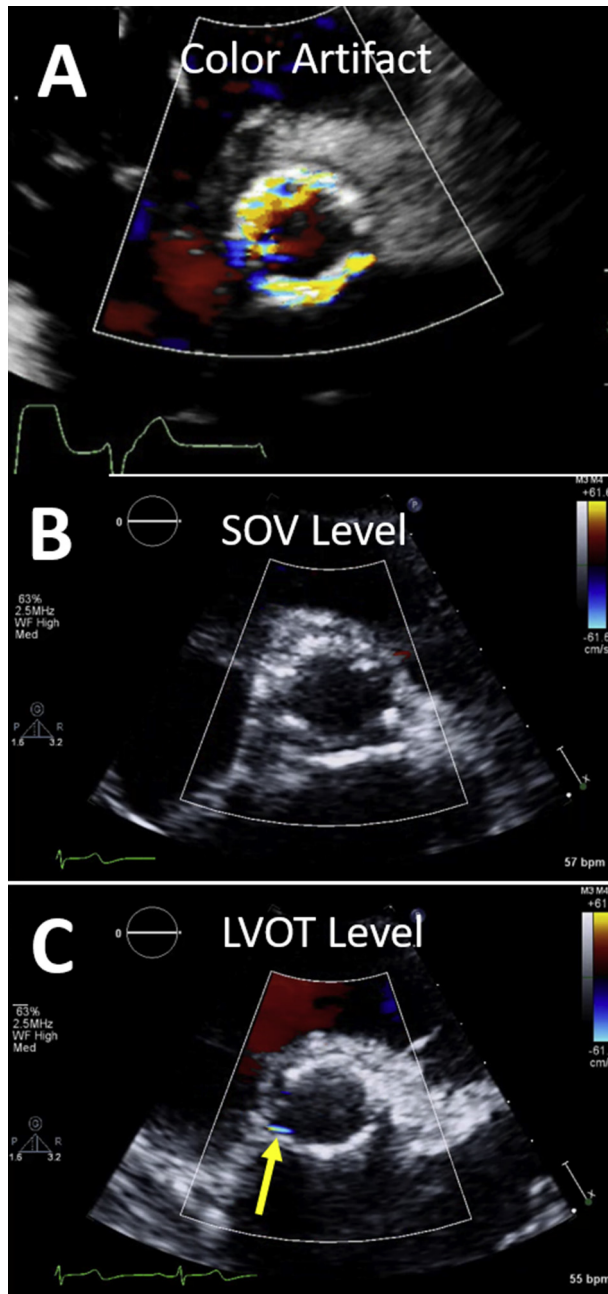


**Figure 8** Imaging of paravalvular aortic regurgitation. Paravalvular aortic regurgitation should be assessed by multiple parameters, and from multiple imaging planes. Panel (A) is the short-axis view showing that the regurgitant jet likely arises from the commissure between the left and noncoronary cusps (*white arrow*). Panel (B) is the long-axis view imaging the proximal convergence zone (*white arrow*) and panel (C) is the transgastric view with the jet area well-imaged. Importantly, the severity of regurgitation should not be assessed by jet area or length. The relatively short pressure half-time (D) can be a result of abnormal ventricular or aortic compliance and is less diagnostic in this patient population.

from distal (aortic) to proximal (ventricular) ends of the THV to identify jet locations and direction. Central prosthetic AR jets will occur at the level of leaflet coaptation, whereas paravalvular regurgitation will be seen at the proximal (ventricular) edge of the THV. Multiple short-axis views with images adjusted to yield the highest frame rates should include the LVOT immediately proximal to the stent (to confirm that jets reach the left ventricle; [Figure 9](#)).

A major limitation of assessment of PAR in the short-axis views of the transcatheter valve with 2D imaging and color flow Doppler, be it by TTE or TEE, is that the scan plane may not be at the level of the origin of the regurgitation; too low (ventricular) a scan plane will overestimate

the severity of regurgitation by imaging jet spray, while too high (aortic) a position may mistake flow in the sinuses of Valsalva for regurgitation. Compared with TTE, TEE provides not only higher quality 2D images but also high-quality 3D color Doppler data sets, which allow planimetry of the vena contracta area ([Figure 10](#)). Three-dimensional TEE has also provided more insight into some of the risk factors associated with transvalvular regurgitation. [Shibayama et al.<sup>154</sup>](#) showed that a more elliptical shape of the prosthetic valve at the commissural level, a larger prosthetic expansion, and antianatomic orientation of the prosthetic valve (prosthetic valve commissures at  $\geq 60^\circ$  compared with the native aortic valve commissures) were associated with transvalvular regurgitation. If



**Figure 9** Imaging of PAR. Color Doppler “twinkling artifact” is seen over the entire metal frame of the transcatheter valve in systole (as well as diastole). **(A)** Multiple short-axis views with images adjusted to yield the highest frame rates should sweep from the midtranscatheter valve **(B)** to assess for central regurgitation, as well as the LVOT immediately proximal to the stent **(C)** to confirm that jets reach the left ventricle. SOV, Sinuses of Valsalva.

the imaging plane is above the stent, regurgitation may not be visualized, or color flow within the sinuses of Valsalva just above the annulus may be mistaken for regurgitant jets below the transcatheter valve. In addition, color Doppler “twinkling artifacts”<sup>155</sup> occur over strongly reflective surfaces such as the metal frame of the transcatheter valve and can be mistaken for regurgitation; these artifacts are pancyclic, and spectral Doppler of these color signals will show nonphysiologic signals (Figure 9A).

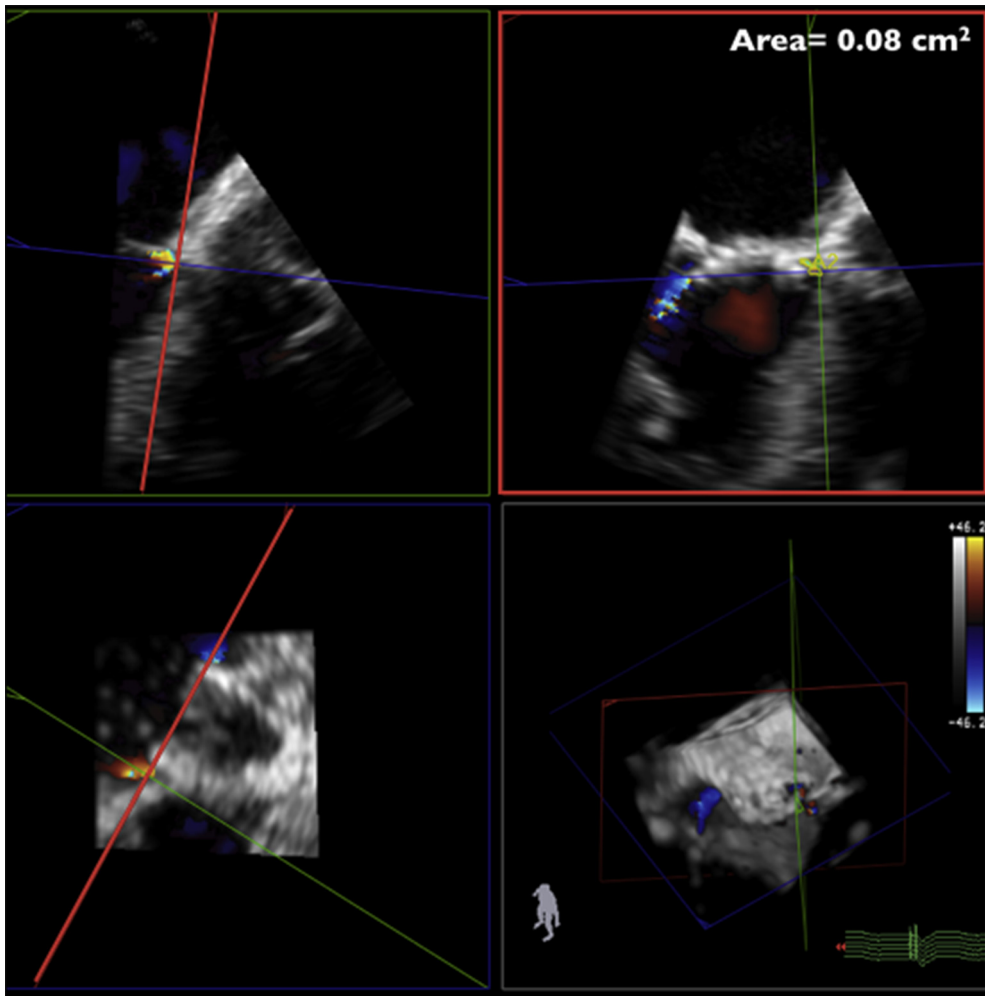
A multiparametric and multiwindow approach based on the integration of multiple indices has been proposed by the Valve Academic Research Consortium (VARC) 2 for the assessment of PAR with a recommendation for a three-class scheme (mild, moderate, and severe).<sup>156</sup> In a series of 1,255 consecutive 2D transthoracic echocardiographic examinations from five TAVR registries, a combination of the VARC-2 parameters was feasible in only 53% of the cases. In 40% of cases, AR after TAVR was graded on the basis of a single reliable VARC-2 criterion supported by non-VARC parameters, and in 7% of cases, post-TAVR AR was graded on the basis of non-VARC parameters.<sup>157</sup> Several other studies have raised the same concern of inconsistencies and variability in assessment of PAR across different core laboratories and between different studies,<sup>158,159</sup> particularly given the limitations of echocardiography (Table 7).

To improve overall feasibility and accuracy in grading PAR, a unifying five-class scheme using qualitative, semiquantitative and quantitative parameters that have emerged from trials and guidelines has been proposed (Table 8).<sup>160</sup> This more granular scheme would ensure more flexibility for the “between-grades” regurgitation jets but would also allow collapsibility and reporting within the three-class scheme recommended by VARC-2: mild and mild to moderate would become mild, and moderate and moderate to severe would become moderate. The ability of this grading scheme to predict outcomes after TAVR has recently been studied. In a retrospective, single-center study, Jones *et al.* found an apparent stepwise increase in mortality for each grade of AR at 1 year, even after controlling for age, gender, Society of Thoracic Surgeons score, baseline LVEF, and AR before TAVR, with a unit HR of 2.26 for each 1+ increase in AR after TAVR (95% CI, 1.48–3.43;  $P < .001$ ). There was a twofold increase in mortality at 1 year for patients with mild AR (1+ and 1 to 2+) compared with those with trivial to 1+ AR.<sup>161</sup> The PARTNER II trial also used the grading scheme and showed that mild and mild to moderate PAR was not associated with worse outcomes compared with no or trace PAR.<sup>162</sup>

A summary of the elements of a comprehensive postprocedural examination is presented in Table 9. Although most aortic root injuries are catastrophic, some are insidious, with slow accumulation of a pericardial effusion and delayed presentation with tamponade physiology.<sup>163</sup> A high level of alertness and suspicion for excluding structural injury as a cause of hemodynamic instability is required at all stages of the procedure. Postprocedural iatrogenic ventricular septal defect has been described, and routine interrogation of the interventricular septum, particularly at the perimembranous level, should be performed.<sup>164</sup>

## PROCEDURAL AND POSTPROCEDURAL IMAGING WITH TTE

Although the initial TAVR trials mandated use of general anesthesia (GA) and intraprocedural TEE, the standardization of the procedure has led to the use of other forms of anesthesia. Sedation without intubation can be performed with an anesthesiologist (monitored anesthetic care) or without (conscious sedation [CS], also known as the “minimalist approach”).<sup>165,166</sup> These approaches limit the ability to perform intraprocedural TEE and rely instead on TTE.<sup>167</sup> The advantages and disadvantages of TTE versus TEE are listed in Table 10.<sup>168</sup> The benefits of this new approach have included lower use of intensive care units, shorter length of stay, and lower cost. This must be weighed against the reports of possible



**Figure 10** Three-dimensional data set of the PAR imaged in Figure 8. Multiplanar reconstruction allows the alignment of the short axis of the vena contracta (*red plane*), which can be planimetered for an estimate of regurgitant severity. In this case, despite the pressure half-time of 258 msec, this jet represents mild paravalvular regurgitation.

**Table 7** Limitations of echocardiographic techniques and parameters for assessing paravalvular regurgitation

Echocardiographic parameters	Pitfalls
Structural parameters <ul style="list-style-type: none"> <li>• Depth of implantation (ME AV LAX, TG LAX, deep TG five-chamber view)</li> <li>• Configuration of the deployed valve (ME AV SAX)</li> </ul>	<ul style="list-style-type: none"> <li>• Presence of artifacts (e.g., acoustic shadowing, side lobe)</li> <li>• Unclear location of the imaging plane in the short-axis views (e.g., too ventricular or too aortic)</li> </ul>
Color Doppler parameters (ME AV LAX, TG LAX, deep TG five-chamber, ME AV SAX) <ul style="list-style-type: none"> <li>• Vena contracta width</li> <li>• Vena contracta area</li> <li>• Circumferential extent</li> </ul>	<ul style="list-style-type: none"> <li>• Multiple jets with origins at different levels</li> <li>• Eccentric jets, tangential to the aortic annular plane</li> <li>• Presence of artifacts (e.g., twinkling, acoustic shadowing)</li> <li>• Unclear location of the imaging plane in short axis (e.g., too ventricular or too aortic)</li> <li>• Irregularity of the regurgitation orifice</li> </ul>
Doppler and quantitative parameters <ul style="list-style-type: none"> <li>• Pressure half-time</li> <li>• Aortic holodiastolic reversal of flow</li> <li>• Regurgitant volume</li> <li>• Regurgitant fraction</li> </ul>	<ul style="list-style-type: none"> <li>• Dependent on ventricular and aortic compliance</li> <li>• Dependent on heart rate and systemic blood pressure</li> <li>• Significant inter- and intraobserver variability for quantitative parameters</li> </ul>
3D imaging	<ul style="list-style-type: none"> <li>• Highly dependent on operator experience</li> <li>• Low spatial and temporal resolution, especially for 3D color data sets</li> </ul>

LAX, Long-axis; ME, midesophageal; SAX, short-axis; TG, transgastric.

**Table 8** Unifying scheme for grading the severity of paravalvular regurgitation

Three-class grading scheme	Trace		Mild		Moderate		Severe
Unifying five-class grading scheme	Trace	Mild	Mild to moderate	Moderate	Moderate to severe	Severe	
<b>Cine angiography</b>							
	Grade 1	Grade 1	Grade 1	Grade 2	Grade 3	Grade 4	
<b>Invasive hemodynamics</b>							
AR index <sup>†</sup>	>25	>25	>25	10–25	10–25	<10	
<b>Doppler echocardiography</b>							
<b>Structural parameters</b>							
• Valve stent	Usually normal	Usually normal	Normal/abnormal <sup>†</sup>	Normal/abnormal <sup>†</sup>	Usually abnormal <sup>†</sup>	Usually abnormal <sup>†</sup>	
◦ LV size <sup>§</sup>	Normal	Normal	Normal	Normal/mildly dilated	Mildly/moderately dilated	Moderately/severely dilated	
<b>Doppler parameters (qualitative or semiquantitative)</b>							
• Jet features							
Extensive/wide jet origin	Absent	Absent	Absent	Present	Present	Present	
Multiple jets	Possible	Possible	Often present	Often present	Usually present	Usually present	
Jet path visible along the stent	Absent	Absent	Possible	Often present	Usually present	Present	
Proximal flow convergence visible	Absent	Absent	Absent	Possible	Often present	Often present	
◦ Vena contracta width (mm)*: color Doppler	<2	<2	2–4	4–5	5–6	>6	
◦ Vena contracta area (mm <sup>2</sup> ) <sup>  </sup> : 3D color Doppler	<5	5–10	10–20	20–30	30–40	>40	
• Jet width at its origin (%LVOT diameter): color Doppler*	Narrow (<5)	Narrow (5–15)	Intermediate (15–30)	Intermediate (30–45)	Large (45–60)	Large (>60)	
◦ Jet density: CW Doppler	Incomplete or faint	Incomplete or faint	Variable	Dense	Dense	Dense	
◦ Jet deceleration rate (PHT, msec): CW Doppler <sup>†,§</sup>	Slow (>500)	Slow (>500)	Slow (>500)	Variable (200–500)	Variable (200–500)	Steep (<200)	
◦ Diastolic flow reversal in the descending aorta: PW Doppler <sup>†,§</sup>	Absent	Absent or brief early diastolic	Intermediate	Intermediate	Holodiastolic (end-diastolic velocity > 20 cm/sec)	Holodiastolic (end-diastolic velocity > 25 cm/sec)	

(Continued)

• Circumferential extent of PAR (%): color Doppler	<10	<10	10–20	20–30	>30	>30
Doppler parameters (quantitative)						
◦ Regurgitant fraction (%)	<15	<15	15–30	30–40	40–50	>50
◦ Effective regurgitant orifice area (mm <sup>2</sup> ) <sup>†</sup>	<5	<5	5–10	10–20	20–30	>30

CW, Continuous-wave; PHT, pressure half-time; PW, pulsed-wave.

Source: Pibarot *et al.*<sup>160</sup>

• Parameters that are most frequently applicable and used to grade PAR severity by echocardiography.

◦ Parameters that are less often applicable because of pitfalls in the feasibility or accuracy of the measurements and/or to the interaction with other factors.

\*These parameters are generally assessed visually.

†Abnormalities of stent position (too low or too high), deployment, and/or circularity.

‡These parameters are influenced by LV and aortic compliance. Hence, low transvalvular end-diastolic aorta-to-LV pressure gradient due to concomitant moderate or severe LV diastolic dysfunction may lead to false-positive results. The high dependency of aortic flow reversal on aortic compliance considerably limits the utility of this parameter in the elderly population undergoing TAVR. These parameters are also influenced by chronotropy.

§Applies to chronic PAR but is less reliable for periprocedural or early postprocedural assessment.

||The vena contracta area is measured by planimetry of the vena contracta of the jet(s) on 2D or 3D color Doppler images in the short-axis view.

¶The effective regurgitant orifice area is calculated by dividing the regurgitant volume by the time-velocity integral of the AR flow by CW Doppler.

**Table 9** Comprehensive echocardiographic assessment following TAVR

	Chamber	Transcatheter valve
Structure	<ul style="list-style-type: none"> <li>• LV dimensions and volume, wall thickness, mass</li> <li>• Right ventricular dimensions (diastolic), wall thickness, function</li> </ul>	<ul style="list-style-type: none"> <li>• Position in relation to the annulus</li> <li>• Stability/motion of the transcatheter valve</li> <li>• Expansion/shape and regions of separation from the annulus</li> </ul>
Function	<ul style="list-style-type: none"> <li>• Regional wall motion abnormalities</li> <li>• EF</li> </ul>	<ul style="list-style-type: none"> <li>• Leaflet motion including an assessment of opening as well as closure</li> </ul>
Hemodynamics	<ul style="list-style-type: none"> <li>• LV stroke volume</li> <li>• Right ventricular stroke volume (for PAR assessment)</li> <li>• Pulmonary artery pressure</li> </ul>	<ul style="list-style-type: none"> <li>• Peak transaortic velocity</li> <li>• Peak and mean transaortic gradient</li> <li>• AVA</li> <li>• Regurgitant severity and location</li> </ul>
Other	<ul style="list-style-type: none"> <li>• Concomitant other valve disease</li> </ul>	<ul style="list-style-type: none"> <li>• Impingement or compromise of adjacent anatomic structures</li> </ul>

**Table 10** Strengths and weaknesses of TTE versus TEE

Parameter	TTE	TEE
Sedation during TAVR	<ul style="list-style-type: none"> <li>None required (sedation for procedure only)</li> </ul>	<ul style="list-style-type: none"> <li>GA, monitored anesthetic care or CS</li> </ul>
Imaging advantages	<ul style="list-style-type: none"> <li>Standard windows for assessing ventricular and valvular structure and function</li> </ul>	<ul style="list-style-type: none"> <li>Higher resolution with high frame rates for 2D and 3D imaging</li> <li>Continuous imaging throughout procedure, irrespective of access route</li> <li>Preprocedural imaging may avoid complications (i.e., paravalvular regurgitation, annular/aortic rupture, coronary occlusion)</li> <li>Immediate intraprocedural diagnosis of complications</li> </ul>
Imaging disadvantages	<ul style="list-style-type: none"> <li>Image quality dependent on patient factors (i.e., chest morphology, lung hyperinflation, suboptimal patient positioning)</li> <li>Procedural delay during image acquisition (to minimize radiation exposure to imager)</li> <li>Noncontinuous imaging during procedure</li> <li>Low resolution with low frame rates for 2D and 3D imaging</li> <li>Limited imaging windows for nontransfemoral access routes</li> </ul>	<ul style="list-style-type: none"> <li>Image quality dependent on patient factors (i.e., calcific acoustic shadowing, cardiac position relative to esophagus and stomach)</li> <li>Probe interference with fluoroscopic imaging (minimized by articulation of probe)</li> </ul>
Other advantages	<ul style="list-style-type: none"> <li>Early recovery and discharge</li> </ul>	<ul style="list-style-type: none"> <li>Need for postprocedural monitoring (may not be different than for TTE)</li> </ul>
Other disadvantages	<ul style="list-style-type: none"> <li>Possible higher radiation exposure to imager</li> <li>Interference with sterile field</li> </ul>	<ul style="list-style-type: none"> <li>Trauma to oropharynx, esophagus, or stomach</li> </ul>

higher paravalvular regurgitation rates,<sup>169,170</sup> nephrotoxic contrast agent use,<sup>171,172</sup> and the increased morbidity of conversion to GA with CS and TEE.<sup>173</sup> Some centers have continued to use GA and TEE but with a “fast track” algorithm that has shortened length of intensive care unit and hospital stays, as well as reduced cost.<sup>174</sup> A Brazilian registry, however, found that the use of TEE to monitor the procedure was a protective factor against overall (HR, 0.57) and late (HR, 0.47) mortality.<sup>175</sup>

Nonetheless, numerous recent reports of the safety of TAVR under monitored anesthetic care or CS<sup>165,176</sup> have resulted in the increasing use of this management protocol.<sup>177</sup> The European Society of Cardiology’s Transcatheter Valve Treatment registry found that survival at 1 year, compared using Kaplan-Meier analysis, was similar between groups (log-rank  $P = .1505$ ), although in the highest tertile logistic European System for Cardiac Operative Risk Evaluation score group, GA patients had higher mortality. Interestingly, GA patients had a higher immediate procedural success rate and a lower rate of periprocedural complications, and CS patients had a strong trend toward higher combined (myocardial infarction, major stroke, and in-hospital death) adverse event rate (7.0% with CS vs 5.3% with GA,  $P = .053$ ).<sup>178</sup>

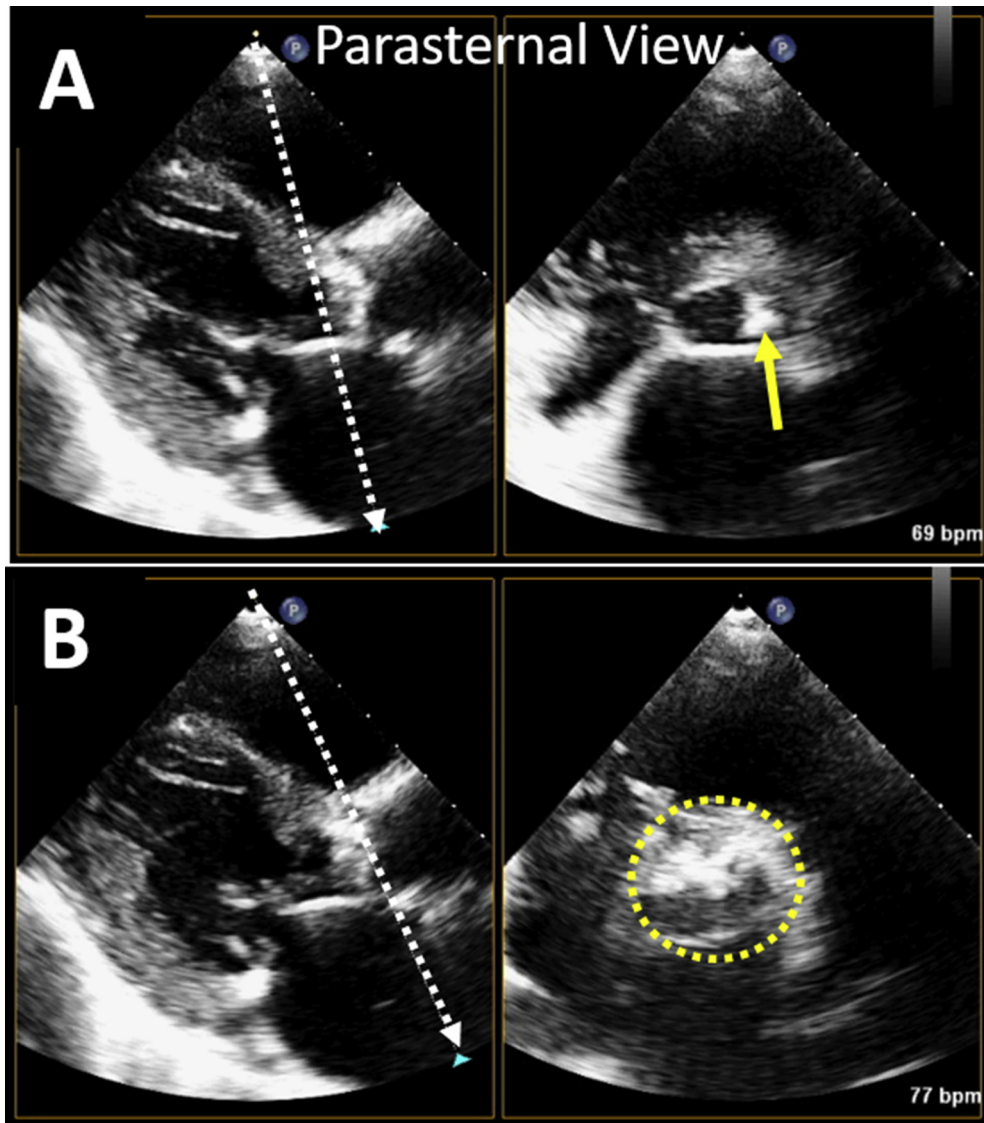
Baseline patient characteristics as well as site experience likely influence the outcomes of the GA and CS approaches. Condado *et al.*<sup>179</sup> studied the GA and CS approaches in patients with chronic obstructive pulmonary disease and showed no differences in procedure complications and 30-day mortality between GA and CS patients with multivariate analysis, showing that the minimalist approach was associated with improved 1-year survival (HR, 0.28; 95% CI, 0.08–0.97). Importantly, similar procedural and short-term outcomes with CS have been seen at some high-volume sites<sup>180</sup>; the first CS procedure in this study was performed after 300 GA studies. Further studies

should be performed as the field begins to address TAVR in the lower risk patient population, who are also at lower risk for GA complications and whose expected outcomes are significantly better than patients treated in these registries.<sup>2,148</sup>

### Transthoracic Echocardiography

Immediate and accurate interpretation of transthoracic echocardiographic images typically requires the presence of a physician echocardiographer in a TAVR suite. Proper training and experience in performing these studies is mandatory.<sup>168</sup> All transthoracic imaging requires direct placement of the probe within the fluoroscopic imaging plane, with possible high exposure to radiation; a team approach is thus needed, because TTE should not be performed during simultaneous fluoroscopy. A standard imaging protocol should be followed if time permits, but frequently a limited, focused study is warranted.

**Baseline Transthoracic Assessment.** A standard imaging protocol should assess ventricular size and function and valvular function (aortic, mitral, tricuspid, and pulmonic). Baseline assessment of cardiac function is essential to identify ideal imaging windows and allow assessment of changes following the procedure or during hemodynamic compromise. The supine position and avoidance of the sterile field may prohibit proper transducer placement, and a “low” parasternal window may be necessary (Figure 11). Although a low parasternal view is not recommended for measurements of the left ventricle, in the elderly population it is frequently ideal for imaging the LVOT, annulus, and aortic root. The use of simultaneous multiplane imaging can be helpful, but the significantly reduced frame rates with this 3D imaging modality may limit its utility for color Doppler assessment of flow. The usual ultrasound



**Figure 11** Transthoracic imaging at baseline from the parasternal long-axis window. **(A)** Simultaneous biplane image from a “low window” imaging plane commonly seen with the patient supine. The orthogonal short-axis view at the level of the LVOT shows bulky calcium (*yellow arrow*) protruding into this space. **(B)** Use of simultaneous multiplane imaging of the aortic valve (*yellow circle*) with very bulky calcification of the right coronary cusp. The *dashed white arrow* on the long-axis (left) view shows the level of imaging for the orthogonal short-axis (right) view.

interference rules still apply, such as chest wall deformities, emphysema, and obesity. In addition, parasternal windows may be limited for assessment of PAR in the setting of posterior annulus shadowing by the THV and the direction of the regurgitant jet perpendicular to the ultrasound beam.

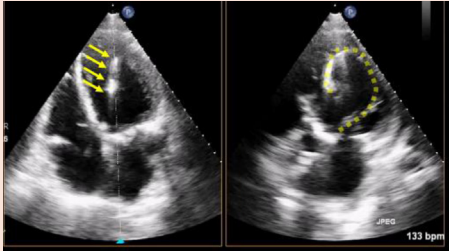
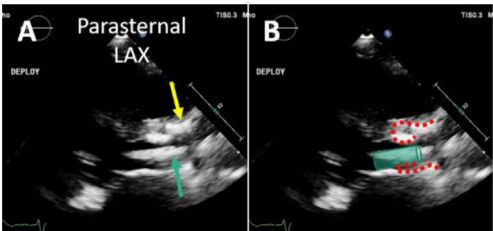
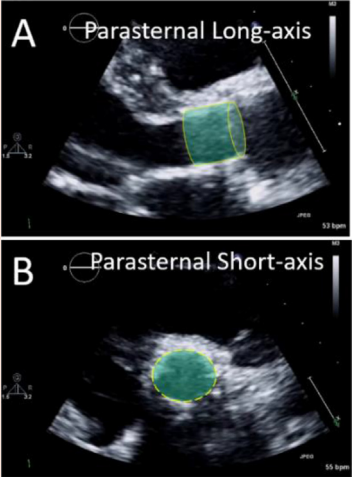
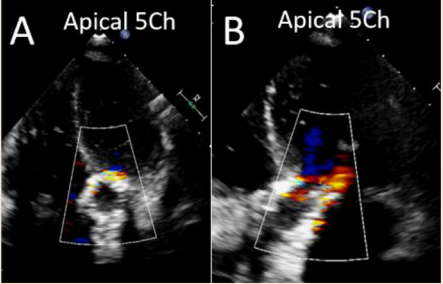
**Intraprocedural Assessment.** Imaging during valve implantation can be performed if the imager and interventionalists work together to eliminate unnecessary radiation exposure to the imager. [Table 11](#) summarizes the transthoracic echocardiographic imaging recommendations during TAVR. It is possible to image wires, catheters, and the stented valve; thus, on occasion, TTE may be used to confirm the position of the stiff wire, pacing wire, or even transcatheter valve.

Immediately after valve deployment, TAVR stent positioning, shape, and leaflet motion can rapidly be assessed with imaging in

biplane mode. The parasternal long-axis view is best for determining the final valve position, but the short-axis view is essential in the assessment of valve shape as well as presence and severity of paravalvular and central AR, as previously discussed. LV and right ventricular wall motion should be carefully assessed from parasternal and apical views; changes in function that correlate with a coronary distribution may indicate an acute coronary obstruction. Apical views are also essential for a full hemodynamic assessment of the THV.

There are a number of caveats to assessing PAR severity intra-procedurally using TTE. First, color Doppler jet length and area, as well as spectral Doppler pressure half-time (by continuous-wave Doppler) or holodiastolic reversal of flow in the descending aorta (by pulsed-wave Doppler), are significantly influenced by blood pressure, LV compliance, and aortic compliance. In this elderly population of patients with severe AS, a noncompliant aorta as

**Table 11** Summary of intraprocedural transthoracic echocardiographic imaging recommendations for TAVR

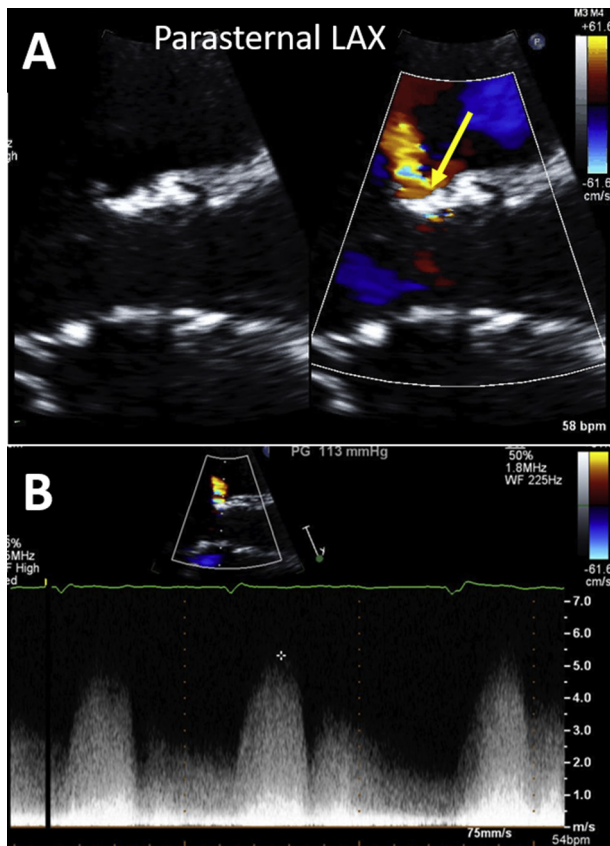
Procedural step	Imaging recommendations	Example
Stiff wire position	<ol style="list-style-type: none"> <li>1. Imaging of wire: ensure stable position in the ventricle without entanglement in mitral apparatus/worsening MR</li> <li>2. Exclude perforation and pericardial effusion</li> </ol>	<p>Simultaneous biplane imaging of the wire (<i>yellow arrows and dashed line</i>)</p> 
Positioning of transcatheter valve	<ol style="list-style-type: none"> <li>1. Balloon-expandable valve               <ol style="list-style-type: none"> <li>a. SAPIEN 3: outflow edge of the transcatheter valve should cover the native leaflets while being below the sinotubular junction; optimal final position covers the native leaflets</li> </ol> </li> <li>2. Self-expanding valve               <ol style="list-style-type: none"> <li>a. EvolutPro: edge of the proximal stent should be 2–4 mm below the annulus</li> </ol> </li> </ol>	<p>The same parasternal LAX image is shown with the crimped SAPIEN 3 valve (<i>green arrow in A and green cylinder in B</i>) below the sinotubular junction (<i>yellow arrow in A</i>) but covering the leaflets (<i>red dashed lines in B</i>)</p> 
Immediate postdeployment	<ol style="list-style-type: none"> <li>1. Assess stent positioning, shape and leaflet motion; perform comprehensive hemodynamic measurements including effective orifice area</li> <li>2. Assess paravalvular regurgitation using short-axis images of the LVOT just apical to the inflow edge of the valve, as well as apical views, to confirm jet reaches the ventricle; note that paravalvular jet length and area are not used to assess severity of regurgitation but may be useful to identify the location and number of regurgitant jets</li> <li>3. Exclude complications (see <a href="#">Table 12</a>)</li> </ol>	 <p>Post-TAVR parasternal imaging of the new THV from long-axis (A) and short-axis (B) views</p>
		 <p>Apical views of the transcatheter valve avoids the shadowing that may limit paravalvular regurgitation assessment from parasternal views</p>

LAX, Long-axis.

**Table 12** Complications of TAVR diagnosed by TTE

Complication	Transthoracic echocardiographic assessment
<b>Hemodynamic instability</b>	
a. Severe transvalvular or PAR	<ul style="list-style-type: none"> <li>Assess location of regurgitation (central vs paravalvular)</li> <li>Assess position of the transcatheter valve</li> <li>Assess severity of AR</li> </ul>
b. Severe MR	<ul style="list-style-type: none"> <li>Evaluate severity of MR and anatomy of the mitral apparatus: valvular perforation, rupture chordae, tethering of the leaflets</li> </ul>
c. Pericardial effusion	<ul style="list-style-type: none"> <li>Assess for tamponade physiology and possible etiology (i.e., chamber perforation, aortic dissection)</li> </ul>
d. Ventricular dysfunction	<ul style="list-style-type: none"> <li>Evaluate for regional or global wall motion abnormalities of the left or right ventricle</li> <li>Identify the coronary ostium; use color flow Doppler to assess blood flow</li> </ul>
e. Aortic rupture or dissection	<ul style="list-style-type: none"> <li>Examine the aortic root/ascending aorta for periaortic hematoma, aortic dissection, or rupture</li> <li>Assess for pericardial effusion/tamponade</li> </ul>
f. Major bleeding	<ul style="list-style-type: none"> <li>Assess ventricular size and function (wall collapse due to hypovolemia)</li> </ul>
<b>Other procedural complications</b>	
a. Identify thrombus on wires/catheters	<ul style="list-style-type: none"> <li>When noted, supplemental heparin may be given</li> </ul>
b. Malpositioning of the THV	<ul style="list-style-type: none"> <li>Too high or too low within the annulus with resulting hemodynamic instability: rapid deployment of a second valve can be performed</li> <li>Embolization of the valve (into the left ventricle or into the aorta) may require surgical intervention</li> </ul>
c. Fistula/perforation	<ul style="list-style-type: none"> <li>Ventricular septal defect</li> <li>Aortocameral fistula (typically into the RVOT or right atrium)</li> </ul>

RVOT, Right ventricular outflow tract.

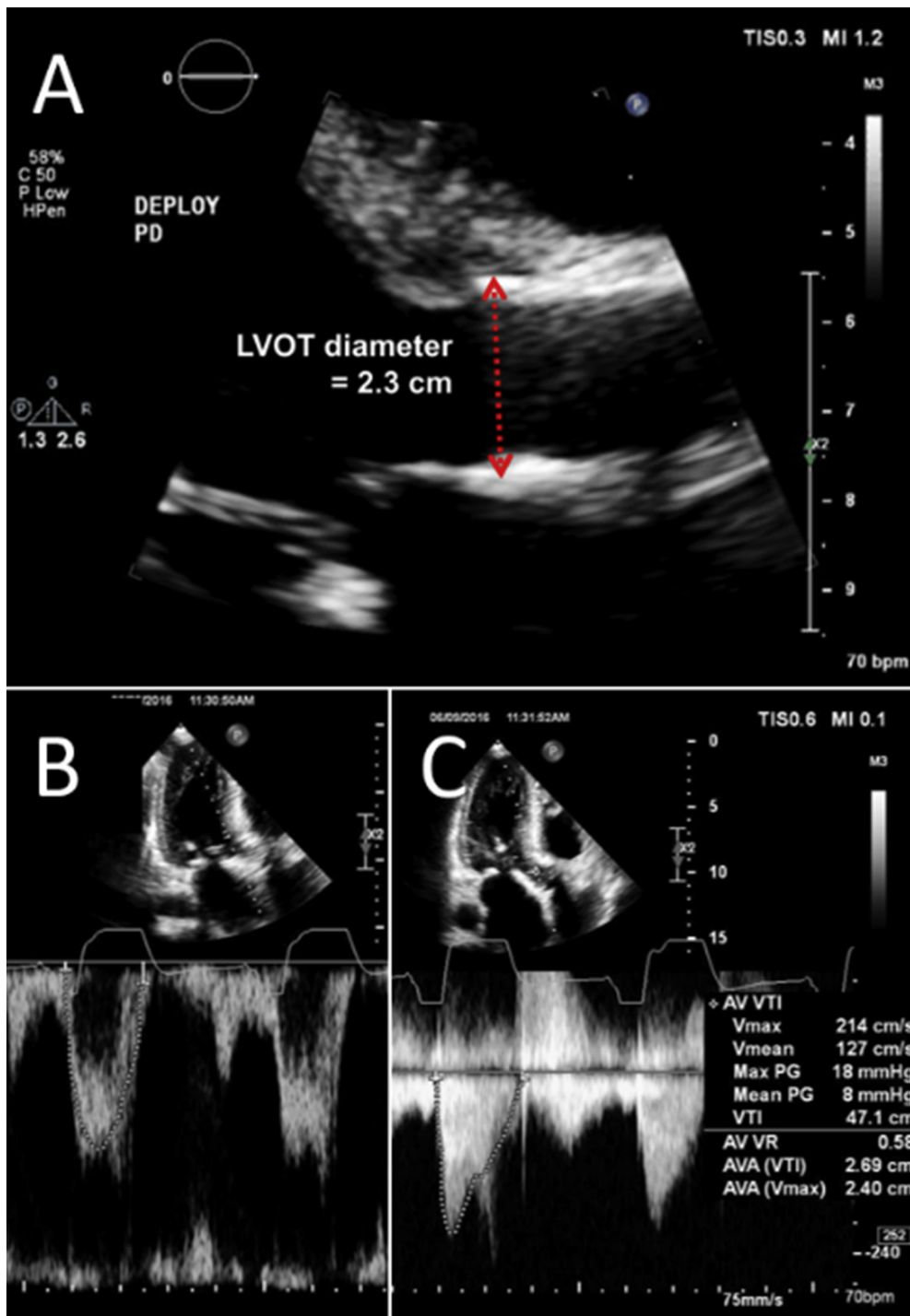


**Figure 12** Acute ventricular septal rupture. **(A)** Two-dimensional and simultaneous color Doppler image of the parasternal long-axis (LAX) view with turbulent color Doppler flow across the membranous septum (yellow arrow). The continuous-wave Doppler signal **(B)** shows pancyclic, high-velocity flow.

well as hypertrophied ventricle may preclude the use of standard measures of aortic regurgitant severity. For instance, large regurgitant volumes ( $\geq 60$  mL) may be seen in chronic severe AR with a dilated ventricle, but for a small, hypertrophied ventricle, acute severe AR may be defined as a much smaller regurgitant volume. Second, the atypical and irregular nature of the PAR jets may limit the accuracy of qualitative, semiquantitative, and quantitative parameters used for native or surgical valve disease and thus change the approach and severity grading. Third, proprietary valve designs may require design-dependent imaging algorithms to assess PAR or valve function.

Other complications of TAVR have been extensively reviewed for both the balloon-expandable and self-expanding valves.<sup>151,152</sup> Importantly, intraprocedural TTE can also rule out the causes of acute hemodynamic compromise listed in Table 12. Other complications, such as perforations (Figure 12), occur rarely<sup>152</sup> but can be easily detected on 2D and Doppler imaging.

**Postprocedural Assessment.** A comprehensive evaluation of chamber and valvular morphology and function should be performed after TAVR (Table 9). An accurate calculation of post-TAVR valve area requires a measurement of LVOT stroke volume.<sup>181,182</sup> Because of flow acceleration within the balloon-expandable stented valve,<sup>181</sup> the LVOT diameter should be measured from the outer to outer stent frame with the pulsed-wave Doppler sample volume placed just apical to the proximal edge of the stent (Figure 13, Table 2). This diameter measurement has been shown to correlate best with measurements of mean gradient.<sup>182</sup> Continuous-wave Doppler across the THV is performed to confirm gradients and calculate valve area. If the LVOT diameter cannot be accurately measured, the Doppler velocity index is recorded and may be a useful measurement for long-term follow-up of valve function. Recent reports of the PARTNER trial suggest that the Doppler velocity index in normal



**Figure 13** Measuring AVA following TAVR. Because of flow acceleration within the balloon-expandable stented valve, the LVOT diameter should be measured from the outer to outer stent frame (A) with pulsed-wave Doppler sample volume placed just apical to the proximal edge of the stent (B). Continuous-wave Doppler is then used to calculate AVA (C).

balloon-expandable valve should be  $>0.45$ .<sup>146</sup> If the stent protrudes into the LVOT cavity (failing to make contact with surrounding tissue), particularly if flow is seen around the outside of inflow stent, then stroke volume measurements using this region of the THV may be invalid. The inner to inner stent diameter at the level of the prosthetic leaflet hinge points can be used with the pulsed-wave Doppler at this same level, but given the

flow acceleration, this calculated valve area typically overestimates the true area. Initial studies of the self-expanding valve suggested that the LVOT diameter should be taken from the just below the hinge points of the visible prosthetic leaflets, measuring the inner to inner stent.<sup>183</sup> Recent trials, however, have used the outer to outer edge of the ventricular edge of the transcatheter valve.<sup>153</sup>

## CONCLUSIONS

In 10 short years, TAVR has become standard of care for inoperable, an equivalent option for high-risk patients, and a consideration for intermediate-risk patients with severe symptomatic AS. Understanding the anatomic variability and constraints of the THV for this procedure as well as the importance and value of echocardiographic imaging is important for any member of the heart team taking care of these patients.

## REFERENCES

- Nishimura RA, Otto CM, Bonow RO, Carabello BA, Erwin JP III, Fleisher LA, et al. 2017 AHA/ACC focused update of the 2014 AHA/ACC guideline for the management of patients with valvular heart disease: a report of the American College of Cardiology/American Heart Association Task Force on Clinical Practice Guidelines. *J Am Coll Cardiol* 2017;70:252-89.
- Thourani VH, Kodali S, Makkar RR, Herrmann HC, Williams M, Babaliaros V, et al. Transcatheter aortic valve replacement versus surgical valve replacement in intermediate-risk patients: a propensity score analysis. *Lancet* 2016;387:2218-25.
- Reardon MJ, Van Mieghem NM, Popma JJ, Kleiman NS, Sondergaard L, Mumtaz M, et al. Surgical or transcatheter aortic-valve replacement in intermediate-risk patients. *N Engl J Med* 2017;376:1321-31.
- Spitzer E, Van Mieghem NM, Pibarot P, Hahn RT, Kodali S, Maurer MS, et al. Rationale and design of the Transcatheter Aortic Valve Replacement to Unload the Left Ventricle in Patients with Advanced Heart Failure (TAVR UNLOAD) trial. *Am Heart J* 2016;182:80-8.
- Genereux P, Stone GW, O'Gara PT, Marquis-Gravel G, Redfors B, Giustino G, et al. Natural history, diagnostic approaches, and therapeutic strategies for patients with asymptomatic severe aortic stenosis. *J Am Coll Cardiol* 2016;67:2263-88.
- Kapadia SR, Schoenhagen P, Stewart W, Tuzcu EM. Imaging for transcatheter valve procedures. *Curr Probl Cardiol* 2010;35:228-76.
- Tretter JT, Spicer DE, Mori S, Chikkabyrappa S, Redington AN, Anderson RH. The significance of the interleaflet triangles in determining the morphology of congenitally abnormal aortic valves: implications for noninvasive imaging and surgical management. *J Am Soc Echocardiogr* 2016;29:1131-43.
- Tuzcu EM, Kapadia SR, Schoenhagen P. Multimodality quantitative imaging of aortic root for transcatheter aortic valve implantation: more complex than it appears. *J Am Coll Cardiol* 2010;55:195-7.
- Ribeiro HB, Webb JG, Makkar RR, Cohen MG, Kapadia SR, Kodali S, et al. Predictive factors, management, and clinical outcomes of coronary obstruction following transcatheter aortic valve implantation: insights from a large multicenter registry. *J Am Coll Cardiol* 2013;62:1552-62.
- Husser O, Pellegrini C, Kessler T, Burgdorf C, Thaller H, Mayr NP, et al. Predictors of permanent pacemaker implantations and new-onset conduction abnormalities with the SAPIEN 3 balloon-expandable transcatheter heart valve. *JACC Cardiovasc Interv* 2016;9:244-54.
- Petronio AS, Sinning JM, Van Mieghem N, Zucchelli G, Nickenig G, Bekeredjian R, et al. Optimal implantation depth and adherence to guidelines on permanent pacing to improve the results of transcatheter aortic valve replacement with the Medtronic CoreValve system: the CoreValve Prospective, International, Post-Market ADVANCE-II study. *JACC Cardiovasc Interv* 2015;8:837-46.
- Leon MB, Smith CR, Mack M, Miller DC, Moses JW, Svensson LG, et al. Transcatheter aortic-valve implantation for aortic stenosis in patients who cannot undergo surgery. *N Engl J Med* 2010;363:1597-607.
- Popma JJ, Adams DH, Reardon MJ, Yakubov SJ, Kleiman NS, Heimansohn D, et al. Transcatheter aortic valve replacement using a self-expanding bioprosthesis in patients with severe aortic stenosis at extreme risk for surgery. *J Am Coll Cardiol* 2014;63:1972-81.
- Bauer T, Linke A, Sievert H, Kahlert P, Hambrecht R, Nickenig G, et al. Comparison of the effectiveness of transcatheter aortic valve implantation in patients with stenotic bicuspid versus tricuspid aortic valves (from the German TAVI Registry). *Am J Cardiol* 2014;113:518-21.
- Mylotte D, Lefevre T, Sondergaard L, Watanabe Y, Modine T, Dvir D, et al. Transcatheter aortic valve replacement in bicuspid aortic valve disease. *J Am Coll Cardiol* 2014;64:2330-9.
- Philip F, Faza NN, Schoenhagen P, Desai MY, Tuzcu EM, Svensson LG, et al. Aortic annulus and root characteristics in severe aortic stenosis due to bicuspid aortic valve and tricuspid aortic valves: implications for transcatheter aortic valve therapies. *Catheter Cardiovasc Interv* 2015;86:E88-98.
- Jilaihawi H, Chen M, Webb J, Himbert D, Ruiz CE, Rodes-Cabau J, et al. A bicuspid aortic valve imaging classification for the TAVR era. *JACC Cardiovasc Imaging* 2016;9:1145-58.
- Perlman GY, Blanke P, Webb JG. Transcatheter aortic valve implantation in bicuspid aortic valve stenosis. *Eurointervention* 2016;12:Y42-5.
- Yoon SH, Lefevre T, Ahn JM, Perlman GY, Dvir D, Latib A, et al. Transcatheter aortic valve replacement with early- and new-generation devices in bicuspid aortic valve stenosis. *J Am Coll Cardiol* 2016;68:1195-205.
- Sievers HH, Schmidtke C. A classification system for the bicuspid aortic valve from 304 surgical specimens. *J Thorac Cardiovasc Surg* 2007;133:1226-33.
- Yousef A, Simard T, Webb J, Rodes-Cabau J, Costopoulos C, Kochman J, et al. Transcatheter aortic valve implantation in patients with bicuspid aortic valve: a patient level multi-center analysis. *Int J Cardiol* 2015;189:282-8.
- Vahanian A, Alfieri O, Andreotti F, Antunes MJ, Baron-Esquivias G, Baumgartner H, et al. Guidelines on the management of valvular heart disease (version 2012): the Joint Task Force on the Management of Valvular Heart Disease of the European Society of Cardiology (ESC) and the European Association for Cardio-Thoracic Surgery (EACTS). *Eur J Cardiothorac Surg* 2012;42:S1-44.
- Zamorano JL, Badano LP, Bruce C, Chan KL, Goncalves A, Hahn RT, et al. EAE/ASE recommendations for the use of echocardiography in new transcatheter interventions for valvular heart disease. *J Am Soc Echocardiogr* 2011;24:937-65.
- Hahn RT, Little SH, Monaghan MJ, Kodali SK, Williams M, Leon MB, et al. Recommendations for comprehensive intraprocedural echocardiographic imaging during TAVR. *JACC Cardiovasc Imaging* 2015;8:261-87.
- Ocak I, Lacomis JM, Deible CR, Pealer K, Parag Y, Knollmann F. The aortic root: comparison of measurements from ECG-gated CT angiography with transthoracic echocardiography. *J Thorac Imaging* 2009;24:223-6.
- Brandenburg RO Jr, Tajik AJ, Edwards WD, Reeder GS, Shub C, Seward JB. Accuracy of 2-dimensional echocardiographic diagnosis of congenitally bicuspid aortic valve: echocardiographic-anatomic correlation in 115 patients. *Am J Cardiol* 1983;51:1469-73.
- Michelena HI, Khanna AD, Mahoney D, Margaryan E, Topilsky Y, Suri RM, et al. Incidence of aortic complications in patients with bicuspid aortic valves. *JAMA* 2011;306:1104-12.
- Hahn RT. Color Doppler to differentiate trileaflet from bicuspid aortic stenosis. Available at: <http://www.acc.org/education-and-meetings/image-and-slide-gallery/media-detail?id=22baf62785c4b06a043fd050ce91bc9>. Accessed November 14, 2016.
- Rosenhek R, Binder T, Porenta G, Lang I, Christ G, Schemper M, et al. Predictors of outcome in severe, asymptomatic aortic stenosis. *N Engl J Med* 2000;343:611-7.
- Otto CM, Lind BK, Kitzman DW, Gersh BJ, Siscovick DS. Association of aortic-valve sclerosis with cardiovascular mortality and morbidity in the elderly. *N Engl J Med* 1999;341:142-7.
- Messika-Zeitoun D, Aubry MC, Detaint D, Bielak LF, Peyser PA, Sheedy PF, et al. Evaluation and clinical implications of aortic valve calcification measured by electron-beam computed tomography. *Circulation* 2004;110:356-62.
- Feuchtnner GM, Muller S, Grander W, Alber HF, Bartel T, Friedrich GJ, et al. Aortic valve calcification as quantified with multislice computed tomography predicts short-term clinical outcome in patients with asymptomatic aortic stenosis. *J Heart Valve Dis* 2006;15:494-8.

33. Clavel MA, Pibarot P, Messika-Zeitoun D, Capoulade R, Malouf J, Aggarwal S, et al. Impact of aortic valve calcification, as measured by MDCT, on survival in patients with aortic stenosis: results of an international registry study. *J Am Coll Cardiol* 2014;64:1202-13.
34. Khalique OK, Hahn RT, Gada H, Nazif TM, Vahl TP, George I, et al. Quantity and location of aortic valve complex calcification predicts severity and location of paravalvular regurgitation and frequency of post-dilation after balloon-expandable transcatheter aortic valve replacement. *JACC Cardiovasc Interv* 2014;7:885-94.
35. Feuchtner G, Plank F, Bartel T, Mueller S, Leipsic J, Schachner T, et al. Prediction of paravalvular regurgitation after transcatheter aortic valve implantation by computed tomography: value of aortic valve and annular calcification. *Ann Thorac Surg* 2013;96:1574-80.
36. Aksoy O, Cam A, Agarwal S, Ige M, Yousefzai R, Singh D, et al. Significance of aortic valve calcification in patients with low-gradient low-flow aortic stenosis. *Clin Cardiol* 2014;37:26-31.
37. Clavel MA, Messika-Zeitoun D, Pibarot P, Aggarwal SR, Malouf J, Araoz PA, et al. The complex nature of discordant severe calcified aortic valve disease grading: new insights from combined Doppler echocardiographic and computed tomographic study. *J Am Coll Cardiol* 2013;62:2329-38.
38. Cuff C, Serfaty JM, Cimadevilla C, Laissy JP, Himbert D, Tubach F, et al. Measurement of aortic valve calcification using multislice computed tomography: correlation with haemodynamic severity of aortic stenosis and clinical implication for patients with low ejection fraction. *Heart* 2011;97:721-6.
39. Thaden JJ, Nkomo VT, Suri RM, Maleszewski JJ, Soderberg DJ, Clavel MA, et al. Sex-related differences in calcific aortic stenosis: correlating clinical and echocardiographic characteristics and computed tomography aortic valve calcium score to excised aortic valve weight. *Eur Heart J* 2016;37:693-9.
40. Naoum C, Blanke P, Dvir D, Pibarot P, Humphries K, Webb J, et al. Clinical outcomes and imaging findings in women undergoing TAVR. *JACC Cardiovasc Imaging* 2016;9:483-93.
41. Baumgartner H, Hung J, Bermejo J, Chambers JB, Edvardsen T, Goldstein S, et al. Recommendations on the echocardiographic assessment of aortic valve stenosis: a focused update from the European Association of Cardiovascular Imaging and the American Society of Echocardiography. *J Am Soc Echocardiogr* 2017;30:372-92.
42. Hahn RT, Pibarot P. Accurate measurement of left ventricular outflow tract diameter: comment on the updated recommendations for the echocardiographic assessment of aortic valve stenosis. *J Am Soc Echocardiogr* 2017;30:1038-41.
43. Mehrotra P, Flynn AW, Jansen K, Tan TC, Mak G, Julien HM, et al. Differential left ventricular outflow tract remodeling and dynamics in aortic stenosis. *J Am Soc Echocardiogr* 2015;28:1259-66.
44. Skjaerpe T, Hegrenaes L, Hatle L. Noninvasive estimation of valve area in patients with aortic stenosis by Doppler ultrasound and two-dimensional echocardiography. *Circulation* 1985;72:810-8.
45. LaBounty TM, Miyasaka R, Chetcuti S, Grossman PM, Deeb GM, Patel HJ, et al. Annulus instead of LVOT diameter improves agreement between echocardiography effective orifice area and invasive aortic valve area. *JACC Cardiovasc Imaging* 2014;7:1065-6.
46. Oh JK, Taliencio CP, Holmes DR Jr, Reeder GS, Bailey KR, Seward JB, et al. Prediction of the severity of aortic stenosis by Doppler aortic valve area determination: prospective Doppler-catheterization correlation in 100 patients. *J Am Coll Cardiol* 1988;11:1227-34.
47. Michelena HI, Margaryan E, Miller FA, Eleid M, Maalouf J, Suri R, et al. Inconsistent echocardiographic grading of aortic stenosis: is the left ventricular outflow tract important? *Heart* 2013;99:921-31.
48. Goland S, Trento A, Iida K, Czer LS, De Robertis M, Naqvi TZ, et al. Assessment of aortic stenosis by three-dimensional echocardiography: an accurate and novel approach. *Heart* 2007;93:801-7.
49. Shahgaldi K, Manouras A, Brodin LA, Winter R. Direct measurement of left ventricular outflow tract area using three-dimensional echocardiography in biplane mode improves accuracy of stroke volume assessment. *Echocardiography* 2010;27:1078-85.
50. Jilaihawi H, Doctor N, Kashif M, Chakravarty T, Rafique A, Makar M, et al. Aortic annular sizing for transcatheter aortic valve replacement using cross-sectional 3-dimensional transesophageal echocardiography. *J Am Coll Cardiol* 2013;61:908-16.
51. Khalique OK, Kodali SK, Paradis JM, Nazif TM, Williams MR, Einstein AJ, et al. Aortic annular sizing using a novel 3-dimensional echocardiographic method: use and comparison with cardiac computed tomography. *Circ Cardiovasc Imaging* 2014;7:155-63.
52. Gaspar T, Adawi S, Sachner R, Asmer I, Ganaem M, Rubinshtein R, et al. Three-dimensional imaging of the left ventricular outflow tract: impact on aortic valve area estimation by the continuity equation. *J Am Soc Echocardiogr* 2012;25:749-57.
53. De Vecchi C, Caudron J, Dubourg B, Piroton N, Lefebvre V, Bauer F, et al. Effect of the ellipsoid shape of the left ventricular outflow tract on the echocardiographic assessment of aortic valve area in aortic stenosis. *J Cardiovasc Comput Tomogr* 2014;8:52-7.
54. Clavel MA, Malouf J, Messika-Zeitoun D, Araoz PA, Michelena HI, Enriquez-Sarano M. Aortic valve area calculation in aortic stenosis by CT and Doppler echocardiography. *JACC Cardiovasc Imaging* 2015;8:248-57.
55. Malouf J, Le Tourneau T, Pellikka P, Sundt TM, Scott C, Schaff HV, et al. Aortic valve stenosis in community medical practice: determinants of outcome and implications for aortic valve replacement. *J Thorac Cardiovasc Surg* 2012;144:1421-7.
56. Jander N, Gohlke-Barwolf C, Bahlmann E, Gerdtts E, Boman K, Chambers JB, et al. Indexing aortic valve area by body surface area increases the prevalence of severe aortic stenosis. *Heart* 2014;100:28-33.
57. Tribouilloy C, Bohbot Y, Marechaux S, Debry N, Delpierre Q, Peltier M, et al. Outcome implication of aortic valve area normalized to body size in asymptomatic aortic stenosis. *Circ Cardiovasc Imaging* 2016;9: e005121.
58. Clavel MA, Burwash IG, Pibarot P. Cardiac imaging for assessing low-gradient severe aortic stenosis. *JACC Cardiovasc Imaging* 2017;10:185-202.
59. Shively BK, Charlton GA, Crawford MH, Chaney RK. Flow dependence of valve area in aortic stenosis: relation to valve morphology. *J Am Coll Cardiol* 1998;31:654-60.
60. Bermejo J, Garcia-Fernandez MA, Torrecilla EG, Bueno H, Moreno MM, San Roman D, et al. Effects of dobutamine on Doppler echocardiographic indexes of aortic stenosis. *J Am Coll Cardiol* 1996;28:1206-13.
61. deFilippi CR, Willett DL, Brickner ME, Appleton CP, Yancy CW, Eichhorn EJ, et al. Usefulness of dobutamine echocardiography in distinguishing severe from nonsevere valvular aortic stenosis in patients with depressed left ventricular function and low transvalvular gradients. *Am J Cardiol* 1995;75:191-4.
62. Lin SS, Roger VL, Pascoe R, Seward JB, Pellikka PA. Dobutamine stress Doppler hemodynamics in patients with aortic stenosis: feasibility, safety, and surgical correlations. *Am Heart J* 1998;136:1010-6.
63. Nishimura RA, Grantham JA, Connolly HM, Schaff HV, Higo ST, Holmes DR Jr. Low-output, low-gradient aortic stenosis in patients with depressed left ventricular systolic function: the clinical utility of the dobutamine challenge in the catheterization laboratory. *Circulation* 2002;106:809-13.
64. Monin JL, Monchi M, Gest V, Duval-Moulin AM, Dubois-Rande JL, Gueret P. Aortic stenosis with severe left ventricular dysfunction and low transvalvular pressure gradients: risk stratification by low-dose dobutamine echocardiography. *J Am Coll Cardiol* 2001;37:2101-7.
65. Clavel MA, Fuchs C, Burwash IG, Mundigler G, Dumesnil JG, Baumgartner H, et al. Predictors of outcomes in low-flow, low-gradient aortic stenosis: results of the multicenter TOPAS study. *Circulation* 2008;118(14 suppl):S234-42.
66. Parker JO, Mark AL, Sanghvi VR, West RO, Khaja F. Hemodynamic effects of pacing-induced tachycardia in valvular aortic stenosis. *Can Med Assoc J* 1983;129:38-41.
67. Kadem L, Pibarot P, Dumesnil JG, Mouret F, Garitey V, Durand LG, et al. Independent contribution of left ventricular ejection time to the mean gradient in aortic stenosis. *J Heart Valve Dis* 2002;11:615-23.

68. Kadem L, Dumesnil JG, Rieu R, Durand L-G, Garcia D, Pibarot P. Impact of systemic hypertension on the assessment of aortic stenosis. *Heart* 2005;91:354-61.
69. Little SH, Chan KL, Burwash IG. Impact of blood pressure on the Doppler echocardiographic assessment of severity of aortic stenosis. *Heart* 2007;93:848-55.
70. Eleid MF, Nishimura RA, Sorajja P, Borlaug BA. Systemic hypertension in low-gradient severe aortic stenosis with preserved ejection fraction. *Circulation* 2013;128:1349-53.
71. Barasch E, Fan D, Chukwu EO, Han J, Passick M, Petillo F, et al. Severe isolated aortic stenosis with normal left ventricular systolic function and low transvalvular gradients: pathophysiologic and prognostic insights. *J Heart Valve Dis* 2008;17:81-8.
72. Leong DP, Pizzale S, Haroun MJ, Yazdan-Ashoori P, Ladak K, Sun YY, et al. Factors associated with low flow in aortic valve stenosis. *J Am Soc Echocardiogr* 2016;29:158-65.
73. Pibarot P, Dumesnil JG. Low-flow, low-gradient aortic stenosis with normal and depressed left ventricular ejection fraction. *J Am Coll Cardiol* 2012;60:1845-53.
74. Lancellotti P, Magne J, Donal E, Davin L, O'Connor K, Rosca M, et al. Clinical outcome in asymptomatic severe aortic stenosis: insights from the new proposed aortic stenosis grading classification. *J Am Coll Cardiol* 2012;59:235-43.
75. Okura H, Yoshida K, Hozumi T, Akasaka T, Yoshikawa J. Planimetry and transthoracic two-dimensional echocardiography in noninvasive assessment of aortic valve area in patients with valvular aortic stenosis. *J Am Coll Cardiol* 1997;30:753-9.
76. Blot-Souletie N, Hebrard A, Acar P, Carrie D, Puel J. Comparison of accuracy of aortic valve area assessment in aortic stenosis by real time three-dimensional echocardiography in biplane mode versus two-dimensional transthoracic and transesophageal echocardiography. *Echocardiography* 2007;24:1065-72.
77. Nakai H, Takeuchi M, Yoshitani H, Kaku K, Haruki N, Otsuji Y. Pitfalls of anatomical aortic valve area measurements using two-dimensional transoesophageal echocardiography and the potential of three-dimensional transoesophageal echocardiography. *Eur J Echocardiogr* 2010;11:369-76.
78. Machida T, Izumo M, Suzuki K, Yoneyama K, Kamijima R, Mizukoshi K, et al. Value of anatomical aortic valve area using real-time three-dimensional transoesophageal echocardiography in patients with aortic stenosis: a comparison between tricuspid and bicuspid aortic valves. *Eur Heart J Cardiovasc Imaging* 2015;16:1120-8.
79. Gorlin R, Gorlin SG. Hydraulic formula for calculation of the area of the stenotic mitral valve, other cardiac valves, and central circulatory shunts. *I. Am Heart J* 1951;41:1-29.
80. Saura D, de la Morena G, Flores-Blanco PJ, Oliva MJ, Caballero L, Gonzalez-Carrillo J, et al. Aortic valve stenosis planimetry by means of three-dimensional transesophageal echocardiography in the real clinical setting: feasibility, reliability and systematic deviations. *Echocardiography* 2015;32:508-15.
81. Bonow RO, Carabello BA, Chatterjee K, de Leon AC Jr, Faxon DP, Freed MD, et al. 2008 Focused update incorporated into the ACC/AHA 2006 guidelines for the management of patients with valvular heart disease: a report of the American College of Cardiology/American Heart Association Task Force on Practice Guidelines (Writing Committee to Revise the 1998 Guidelines for the Management of Patients With Valvular Heart Disease): endorsed by the Society of Cardiovascular Anesthesiologists, Society for Cardiovascular Angiography and Interventions, and Society of Thoracic Surgeons. *Circulation* 2008;118:e523-661.
82. Niederberger J, Schima H, Maurer G, Baumgartner H. Importance of pressure recovery for the assessment of aortic stenosis by Doppler ultrasound. Role of aortic size, aortic valve area, and direction of the stenotic jet in vitro. *Circulation* 1996;94:1934-40.
83. Chambers JB, Spriggs DC, Cochrane T, Allen J, Morris R, Black MM, et al. Continuity equation and Gorlin formula compared with directly observed orifice area in native and prosthetic aortic valves. *Br Heart J* 1992;67:193-9.
84. Heinrich RS, Marcus RH, Ensley AE, Gibson DE, Yoganathan AP. Valve orifice area alone is an insufficient index of aortic stenosis severity: effects of the proximal and distal geometry on transaortic energy loss. *J Heart Valve Dis* 1999;8:509-15.
85. Baumgartner H, Hung J, Bermejo J, Chambers JB, Evangelista A, Griffin BP, et al. Echocardiographic assessment of valve stenosis: EAE/ASE recommendations for clinical practice. *J Am Soc Echocardiogr* 2009;22:1-23.
86. Bahlmann E, Cramariuc D, Gerds E, Gohlke-Baerwolf C, Nienaber CA, Eriksen E, et al. Impact of pressure recovery on echocardiographic assessment of asymptomatic aortic stenosis: a SEAS substudy. *JACC Cardiovasc Imaging* 2010;3:555-62.
87. Garcia D, Dumesnil JG, Durand LG, Kadem L, Pibarot P. Discrepancies between catheter and Doppler estimates of valve effective orifice area can be predicted from the pressure recovery phenomenon: practical implications with regard to quantification of aortic stenosis severity. *J Am Coll Cardiol* 2003;41:435-42.
88. Briand M, Dumesnil JG, Kadem L, Tongue AG, Rieu R, Garcia D, et al. Reduced systemic arterial compliance impacts significantly on left ventricular afterload and function in aortic stenosis: implications for diagnosis and treatment. *J Am Coll Cardiol* 2005;46:291-8.
89. Hachicha Z, Dumesnil JG, Pibarot P. Usefulness of the valvuloarterial impedance to predict adverse outcome in asymptomatic aortic stenosis. *J Am Coll Cardiol* 2009;54:1003-11.
90. Antonini-Canterin F, Huang G, Cervesato E, Faggiano P, Pavan D, Piazza R, et al. Symptomatic aortic stenosis: does systemic hypertension play an additional role? *Hypertension* 2003;41:1268-72.
91. Lancellotti P, Donal E, Magne J, Moonen M, O'Connor K, Daubert JC, et al. Risk stratification in asymptomatic moderate to severe aortic stenosis: the importance of the valvular, arterial and ventricular interplay. *Heart* 2010;96:1364-71.
92. Marechaux S, Carpentier E, Six-Carpentier M, Asseman P, Lejemtel TH, Jude B, et al. Impact of valvuloarterial impedance on left ventricular longitudinal deformation in patients with aortic valve stenosis and preserved ejection fraction. *Arch Cardiovasc Dis* 2010;103:227-35.
93. Herrmann S, Stork S, Niemann M, Lange V, Strotmann JM, Frantz S, et al. Low-gradient aortic valve stenosis myocardial fibrosis and its influence on function and outcome. *J Am Coll Cardiol* 2011;58:402-12.
94. Garbi M, Chambers J, Vannan MA, Lancellotti P. Valve stress echocardiography: a practical guide for referral, procedure, reporting, and clinical implementation of results from the HAVEC group. *J Am Coll Cardiol* 2015;8:724-36.
95. Ross J Jr, Braunwald E. Aortic stenosis. *Circulation* 1968;38(1 suppl):61-7.
96. Nishimura RA, Otto CM, Bonow RO, Carabello BA, Erwin JP III, Guyton RA, et al. 2014 AHA/ACC guideline for the management of patients with valvular heart disease: executive summary: a report of the American College of Cardiology/American Heart Association Task Force on Practice Guidelines. *J Am Coll Cardiol* 2014;63:2438-88.
97. Amato MC, Moffa PJ, Werner KE, Ramires JA. Treatment decision in asymptomatic aortic valve stenosis: role of exercise testing. *Heart* 2001;86:381-6.
98. Marechaux S, Hachicha Z, Bellouin A, Dumesnil JG, Meimoun P, Pasquet A, et al. Usefulness of exercise-stress echocardiography for risk stratification of true asymptomatic patients with aortic valve stenosis. *Eur Heart J* 2010;31:1390-7.
99. Lancellotti P, Lebois F, Simon M, Tombeux C, Chauvel C, Pierard LA. Prognostic importance of quantitative exercise Doppler echocardiography in asymptomatic valvular aortic stenosis. *Circulation* 2005;112(9 suppl):I377-82.
100. Taniguchi T, Morimoto T, Shiomi H, Ando K, Kanamori N, Murata K, et al. Initial surgical versus conservative strategies in patients with asymptomatic severe aortic stenosis. *J Am Coll Cardiol* 2015;66:2827-38.
101. Voigt JU, Pedrizzetti G, Lysyansky P, Marwick TH, Houle H, Baumann R, et al. Definitions for a common standard for 2D speckle tracking

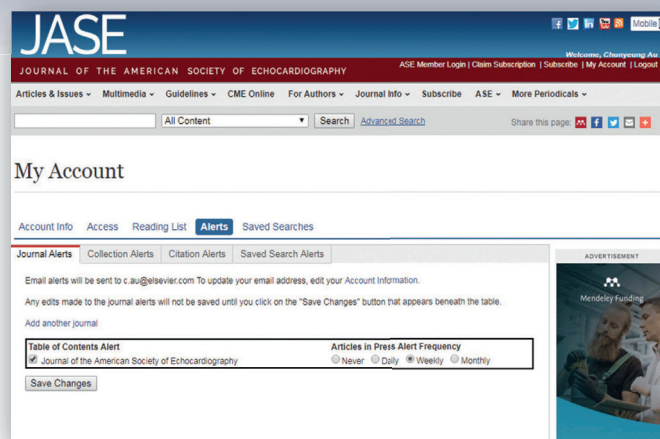
- echocardiography: consensus document of the EACVI/ASE/Industry Task Force to Standardize Deformation Imaging. *Eur Heart J Cardiovasc Imaging* 2015;16:1-11.
102. Rodes-Cabau J, Webb JG, Cheung A, Ye J, Dumont E, Feindel CM, et al. Transcatheter aortic valve implantation for the treatment of severe symptomatic aortic stenosis in patients at very high or prohibitive surgical risk: acute and late outcomes of the multicenter Canadian experience. *J Am Coll Cardiol* 2010;55:1080-90.
  103. Kang D, Bach DS, Chetcuti S, Deeb GM, Grossman PM, Patel HJ, et al. Mortality predictors in patients referred for but not undergoing transcatheter aortic valve replacement. *Am J Cardiol* 2015;116:919-24.
  104. Parikh R, Goodman AL, Barr T, Sabik JF, Svensson LG, Rodriguez LL, et al. Outcomes of surgical aortic valve replacement for severe aortic stenosis: incorporation of left ventricular systolic function and stroke volume index. *J Thorac Cardiovasc Surg* 2015;149:1558-66.e1.
  105. Sannino A, Gargiulo G, Schiattarella GG, Brevetti L, Perrino C, Stabile E, et al. Increased mortality after transcatheter aortic valve implantation (TAVI) in patients with severe aortic stenosis and low ejection fraction: a meta-analysis of 6898 patients. *Int J Cardiol* 2014;176:32-9.
  106. Miyazaki S, Daimon M, Miyazaki T, Onishi Y, Koiso Y, Nishizaki Y, et al. Global longitudinal strain in relation to the severity of aortic stenosis: a two-dimensional speckle-tracking study. *Echocardiography* 2011;28:703-8.
  107. Ng AC, Delgado V, Bertini M, Antoni ML, van Bommel RJ, van Rijnsoever EP, et al. Alterations in multidirectional myocardial functions in patients with aortic stenosis and preserved ejection fraction: a two-dimensional speckle tracking analysis. *Eur Heart J* 2011;32:1542-50.
  108. Kusunose K, Goodman A, Parikh R, Barr T, Agarwal S, Popovic ZB, et al. Incremental prognostic value of left ventricular global longitudinal strain in patients with aortic stenosis and preserved ejection fraction. *Circ Cardiovasc Imaging* 2014;7:938-45.
  109. Kearney LG, Lu K, Ord M, Patel SK, Profitis K, Matalanis G, et al. Global longitudinal strain is a strong independent predictor of all-cause mortality in patients with aortic stenosis. *Eur Heart J Cardiovasc Imaging* 2012;13:827-33.
  110. Dahl JS, Videbaek L, Poulsen MK, Rudbaek TR, Pellikka PA, Moller JE. Global strain in severe aortic valve stenosis: relation to clinical outcome after aortic valve replacement. *Circ Cardiovasc Imaging* 2012;5:613-20.
  111. Kamperidis V, van Rosendaal PJ, Ng AC, Katsanos S, van der Kley F, Debonnaire P, et al. Impact of flow and left ventricular strain on outcome of patients with preserved left ventricular ejection fraction and low gradient severe aortic stenosis undergoing aortic valve replacement. *Am J Cardiol* 2014;114:1875-81.
  112. Dahou A, Bartko PE, Capoulade R, Clavel MA, Mundigler G, Grondin SL, et al. Usefulness of global left ventricular longitudinal strain for risk stratification in low ejection fraction, low-gradient aortic stenosis: results from the multicenter True or Pseudo-Severe Aortic Stenosis study. *Circ Cardiovasc Imaging* 2015;8:e002117.
  113. Nagata Y, Takeuchi M, Wu VC, Izumo M, Suzuki K, Sato K, et al. Prognostic value of LV deformation parameters using 2D and 3D speckle-tracking echocardiography in asymptomatic patients with severe aortic stenosis and preserved LV ejection fraction. *JACC Cardiovasc Imaging* 2015;8:235-45.
  114. Carstensen HG, Larsen LH, Hassager C, Kofoed KF, Jensen JS, Mogelvang R. Association of ischemic heart disease to global and regional longitudinal strain in asymptomatic aortic stenosis. *Int J Cardiovasc Imaging* 2015;31:485-95.
  115. Carasso S, Mutlak D, Lessick J, Reisner SA, Rakowski H, Agmon Y. Symptoms in severe aortic stenosis are associated with decreased compensatory circumferential myocardial mechanics. *J Am Soc Echocardiogr* 2015;28:218-25.
  116. Attias D, Macron L, Dreyfus J, Monin JL, Brochet E, Lepage L, et al. Relationship between longitudinal strain and symptomatic status in aortic stenosis. *J Am Soc Echocardiogr* 2013;26:868-74.
  117. Carstensen HG, Larsen LH, Hassager C, Kofoed KF, Jensen JS, Mogelvang R. Basal longitudinal strain predicts future aortic valve replacement in asymptomatic patients with aortic stenosis. *Eur Heart J Cardiovasc Imaging* 2016;17:283-92.
  118. Logstrup BB, Andersen HR, Thuesen L, Christiansen EH, Terp K, Klaborg KE, et al. Left ventricular global systolic longitudinal deformation and prognosis 1 year after femoral and apical transcatheter aortic valve implantation. *J Am Soc Echocardiogr* 2013;26:246-54.
  119. Biner S, Rafique AM, Goykhan P, Morrissey RP, Naghi J, Siegel RJ. Prognostic value of E/E' ratio in patients with unoperated severe aortic stenosis. *JACC Cardiovasc Imaging* 2010;3:899-907.
  120. Tan TC, Flynn AW, Chen-Tournoux A, Rudski LG, Mehrotra P, Nunes MC, et al. Risk prediction in aortic valve replacement: incremental value of the preoperative echocardiogram. *J Am Heart Assoc* 2015;4:e002129.
  121. Goncalves A, Marcos-Alberca P, Almeria C, Feltes G, Rodriguez E, Hernandez-Antolin RA, et al. Acute left ventricle diastolic function improvement after transcatheter aortic valve implantation. *Eur J Echocardiogr* 2011;12:790-7.
  122. Muratori M, Fusini L, Tamborini G, Gripari P, Delgado V, Marsan NA, et al. Sustained favourable haemodynamics 1 year after TAVI: improvement in NYHA functional class related to improvement of left ventricular diastolic function. *Eur Heart J Cardiovasc Imaging* 2016;17:1269-78.
  123. Caballero-Borrego J, Gomez-Doblas JJ, Cabrera-Bueno F, Garcia-Pinilla JM, Melero JM, Porras C, et al. Incidence, associated factors and evolution of non-severe functional mitral regurgitation in patients with severe aortic stenosis undergoing aortic valve replacement. *Eur J Cardiothorac Surg* 2008;34:62-6.
  124. Unger P, Dedobbeleer C, Van Camp G, Plein D, Cosyns B, Lancellotti P. Republished review: mitral regurgitation in patients with aortic stenosis undergoing valve replacement. *Postgrad Med J* 2011;87:150-5.
  125. Barbanti M, Webb JG, Hahn RT, Feldman T, Boone RH, Smith CR, et al. Impact of preoperative moderate/severe mitral regurgitation on 2-year outcome after transcatheter and surgical aortic valve replacement: insight from the PARTNER (Placement of Aortic Transcatheter Valve) trial cohort A. *Circulation* 2013;128:2776-84.
  126. Nishimura RA, Otto CM, Bonow RO, Carabello BA, Erwin JP III, Guyton RA, et al. 2014 AHA/ACC guideline for the management of patients with valvular heart disease: a report of the American College of Cardiology/American Heart Association Task Force on Practice Guidelines. *Journal of the American College of Cardiology* 2014;63:e57-185.
  127. Holmes DR Jr, Mack MJ, Kaul S, Agnihotri A, Alexander KP, Bailey SR, et al. 2012 ACCF/AATS/SCAI/STS expert consensus document on transcatheter aortic valve replacement. *J Am Coll Cardiol* 2012;59:1200-54.
  128. Achenbach S, Delgado V, Hausleiter J, Schoenhagen P, Min JK, Leipsic JA. SCCT expert consensus document on computed tomography imaging before transcatheter aortic valve implantation (TAVI)/transcatheter aortic valve replacement (TAVR). *J Cardiovasc Comput Tomogr* 2012;6:366-80.
  129. Otto CM, Kumbhani DJ, Alexander KP, Calhoun JH, Desai MY, Kaul S, et al. 2017 ACC expert consensus decision pathway for transcatheter aortic valve replacement in the management of adults with aortic stenosis: a report of the American College of Cardiology Task Force on Clinical Expert Consensus Documents. *J Am Coll Cardiol* 2017;69:1313-46.
  130. Binder RK, Webb JG, Willson AB, Urena M, Hansson NC, Norgaard BL, et al. The impact of integration of a multidetector computed tomography annulus area sizing algorithm on outcomes of transcatheter aortic valve replacement: a prospective, multicenter, controlled trial. *J Am Coll Cardiol* 2013;62:431-8.
  131. Jilaihawi H, Kashif M, Fontana G, Furugen A, Shiota T, Friede G, et al. Cross-sectional computed tomographic assessment improves accuracy of aortic annular sizing for transcatheter aortic valve replacement and reduces the incidence of paravalvular aortic regurgitation. *J Am Coll Cardiol* 2012;59:1275-86.
  132. Gurvitch R, Webb JG, Yuan R, Johnson M, Hague C, Willson AB, et al. Aortic annulus diameter determination by multidetector computed tomography: reproducibility, applicability, and implications for transcatheter aortic valve implantation. *JACC Cardiovasc Interv* 2011;4:1235-45.
  133. Otani K, Takeuchi M, Kaku K, Sugeng L, Yoshitani H, Haruki N, et al. Assessment of the aortic root using real-time 3D transesophageal echocardiography. *Circ J* 2010;74:2649-57.

134. Smith LA, Dworakowski R, Bhan A, Delithanasis I, Hancock J, Maccarthy PA, et al. Real-time three-dimensional transesophageal echocardiography adds value to transcatheter aortic valve implantation. *J Am Soc Echocardiogr* 2013;26:359-69.
135. Altiok E, Koos R, Schroder J, Brehmer K, Hamada S, Becker M, et al. Comparison of two-dimensional and three-dimensional imaging techniques for measurement of aortic annulus diameters before transcatheter aortic valve implantation. *Heart* 2011;97:1578-84.
136. Hahn R, Khalique O, Williams M, Koss E, Paradis J-M, Daneault B, et al. Predicting paravalvular regurgitation following transcatheter valve replacement: utility of a novel method for three-dimensional echocardiographic measurements of the aortic annulus. *J Am Soc Echocardiogr* 2013;26:1044-52.
137. Grasso C, Scandura S, Buccheri S, Barbanti M, Di Salvo ME, Mangiafico S, et al. MitraClip implantation for the treatment of new-onset systolic anterior motion of the mitral valve after transcatheter aortic valve replacement. *Ann Thorac Surg* 2016;102:e517-9.
138. Abdel-Wahab M, Zahn R, Horack M, Gerckens U, Schuler G, Sievert H, et al. Aortic regurgitation after transcatheter aortic valve implantation: incidence and early outcome. Results from the German transcatheter aortic valve interventions registry. *Heart* 2011;97:899-906.
139. Detaint D, Lepage L, Himbert D, Brochet E, Messika-Zeitoun D, Lung B, et al. Determinants of significant paravalvular regurgitation after transcatheter aortic valve: implantation impact of device and annulus congruence. *JACC Cardiovasc Interv* 2009;2:821-7.
140. Ewe SH, Ng AC, Schuijf JD, van der Kley F, Colli A, Palmén M, et al. Location and severity of aortic valve calcium and implications for aortic regurgitation after transcatheter aortic valve implantation. *Am J Cardiol* 2011;108:1470-7.
141. Gotzmann M, Bojara W, Lindstaedt M, Ewers A, Bosche L, Germing A, et al. One-year results of transcatheter aortic valve implantation in severe symptomatic aortic valve stenosis. *Am J Cardiol* 2011;107:1687-92.
142. Moat NE, Ludman P, de Belder MA, Bridgewater B, Cunningham AD, Young CP, et al. Long-term outcomes after transcatheter aortic valve implantation in high-risk patients with severe aortic stenosis: the U.K. TAVI (United Kingdom Transcatheter Aortic Valve Implantation) registry. *J Am Coll Cardiol* 2011;58:2130-8.
143. Piazza N, Schultz C, de Jaegere PP, Serruys PW. Implantation of two self-expanding aortic bioprosthetic valves during the same procedure—Insights into valve-in-valve implantation (“Russian doll concept”). *Catheter Cardiovasc Interv* 2009;73:530-9.
144. Smith CR, Leon MB, Mack MJ, Miller DC, Moses JW, Svensson LG, et al. Transcatheter versus surgical aortic-valve replacement in high-risk patients. *N Engl J Med* 2011;364:2187-98.
145. Ussia GP, Barbanti M, Petronio AS, Tarantini G, Ettore F, Colombo A, et al. Transcatheter aortic valve implantation: 3-year outcomes of self-expanding CoreValve prosthesis. *Eur Heart J* 2012;33:969-76.
146. Hahn RT, Pibarot P, Stewart WJ, Weissman NJ, Gopalakrishnan D, Keane MG, et al. Comparison of transcatheter and surgical aortic valve replacement in severe aortic stenosis: a longitudinal study of echocardiography parameters in cohort A of the PARTNER trial (Placement of Aortic Transcatheter Valves). *J Am Coll Cardiol* 2013;61:2514-21.
147. Oh JK, Little SH, Abdelmoneim SS, Reardon MJ, Kleiman NS, Lin G, et al. Regression of paravalvular aortic regurgitation and remodeling of self-expanding transcatheter aortic valve: an observation from the CoreValve U.S. pivotal trial. *JACC Cardiovasc Imaging* 2015;8:1364-75.
148. Kodali S, Thourani VH, White J, Malaisrie SC, Lim S, Greason KL, et al. Early clinical and echocardiographic outcomes after SAPIEN 3 transcatheter aortic valve replacement in inoperable, high-risk and intermediate-risk patients with aortic stenosis. *Eur Heart J* 2016;37:2252-62.
149. Meredith IT, Walters DL, Dumontel N, Worthley SG, Tchetché D, Manoharan G, et al. 1-Year outcome with the fully repositionable and retrievable Lotus transcatheter aortic replacement valve in 120 high-risk surgical patients with severe aortic stenosis: results of the REPRISE II study. *JACC Cardiovasc Interv* 2016;9:376-84.
150. Popma JJ, Reardon MJ, Khabbaz K, Harrison JK, Hughes GC, Kodali S, et al. Early clinical outcomes after transcatheter aortic valve replacement using a novel self-expanding bioprosthesis in patients with severe aortic stenosis who are suboptimal for surgery: results of the Evolut R U.S. study. *JACC Cardiovasc Interv* 2017;10:268-75.
151. Hahn RT, Gillam LD, Little SH. Echocardiographic imaging of procedural complications during self-expandable transcatheter aortic valve replacement. *JACC Cardiovasc Imaging* 2015;8:319-36.
152. Hahn RT, Kodali S, Tuzcu EM, Leon MB, Kapadia S, Gopal D, et al. Echocardiographic imaging of procedural complications during balloon-expandable transcatheter aortic valve replacement. *JACC Cardiovasc Imaging* 2015;8:288-318.
153. Adams DH, Popma JJ, Reardon MJ, Yakubov SJ, Coselli JS, Deeb GM, et al. Transcatheter aortic-valve replacement with a self-expanding prosthesis. *N Engl J Med* 2014;370:1790-8.
154. Shibayama K, Mihara H, Jilaihawi H, Berdejo J, Harada K, Itabashi Y, et al. 3D assessment of features associated with transvalvular aortic regurgitation after TAVR: a real-time 3D TEE study. *JACC Cardiovasc Imaging* 2016;9:114-23.
155. Le HT, Hangiandreou N, Timmerman R, Rice MJ, Smith WB, Deitte L, et al. Imaging artifacts in echocardiography. *Anesth Analg* 2016;122:633-46.
156. Kappetein AP, Head SJ, Genereux P, Piazza N, van Mieghem NM, Blackstone EH, et al. Updated standardized endpoint definitions for transcatheter aortic valve implantation: the Valve Academic Research Consortium-2 consensus document. *J Am Coll Cardiol* 2012;60:1438-54.
157. Abdelghani M, Spitzer E, Ren B, Serruys PW, Soliman OI. Real-world feasibility of the VARC-recommended multiparametric approach for the assessment of post-TAVI aortic regurgitation. *Int J Cardiol* 2016;223:220-1.
158. Hahn RT, Pibarot P, Weissman NJ, Rodriguez L, Jaber WA. Assessment of paravalvular aortic regurgitation after transcatheter aortic valve replacement: intra-core laboratory variability. *J Am Soc Echocardiogr* 2015;28:415-22.
159. Kodali S, Pibarot P, Douglas PS, Williams M, Xu K, Thourani V, et al. Paravalvular regurgitation after transcatheter aortic valve replacement with the Edwards SAPIEN valve in the PARTNER trial: characterizing patients and impact on outcomes. *Eur Heart J* 2015;36:449-56.
160. Pibarot P, Hahn RT, Weissman NJ, Monaghan MJ. Assessment of paravalvular regurgitation following TAVR: a proposal of unifying grading scheme. *JACC Cardiovasc Imaging* 2015;8:340-60.
161. Jones BM, Tuzcu EM, Krishnaswamy A, Popovic Z, Mick S, Roselli EE, et al. Prognostic significance of mild aortic regurgitation in predicting mortality after transcatheter aortic valve replacement. *J Thorac Cardiovasc Surg* 2016;152:783-890.
162. Pibarot P, Hahn RT, Weissman NJ, et al. Association of paravalvular regurgitation with 1-year outcomes after transcatheter aortic valve replacement with the SAPIEN 3 valve. *JAMA Cardiol* 2017;2:1208-16.
163. Keenan JE, Vavalle JP, Ganapathi AM, Wang H, Harrison JK, Wang A, et al. Factor VIIa for annulus rupture after transcatheter aortic valve replacement. *Ann Thorac Surg* 2015;100:313-5.
164. Ando T, Holmes AA, Taub CC, Slovut DP, DeRose JJ. Iatrogenic ventricular septal defect following transcatheter aortic valve replacement: a systematic review. *Heart Lung Circ* 2016;25:968-74.
165. Babaliaros V, Devireddy C, Lerakis S, Leonardi R, Iturra SA, Mavromatis K, et al. Comparison of transfemoral transcatheter aortic valve replacement performed in the catheterization laboratory (minimalist approach) versus hybrid operating room (standard approach): outcomes and cost analysis. *JACC Cardiovasc Interv* 2014;7:898-904.
166. Durand E, Borz B, Godin M, Tron C, Litzler PY, Bessou JP, et al. Transfemoral aortic valve replacement with the Edwards SAPIEN and Edwards SAPIEN XT prosthesis using exclusively local anesthesia and fluoroscopic guidance: feasibility and 30-day outcomes. *JACC Cardiovasc Interv* 2012;5:461-7.
167. Dvir D, Jhaveri R, Pichard AD. The minimalist approach for transcatheter aortic valve replacement in high-risk patients. *JACC Cardiovasc Interv* 2012;5:468-9.
168. Kronzon I, Jelnin V, Ruiz CE, Saric M, Williams MR, Kasel AM, et al. Optimal imaging for guiding TAVR: transesophageal or transthoracic echocardiography, or just fluoroscopy? *JACC Cardiovasc Imaging* 2015;8:361-70.

169. Oguri A, Yamamoto M, Mouillet G, Gilard M, Laskar M, Eltchaninoff H, et al. Clinical outcomes and safety of transfemoral aortic valve implantation under general versus local anesthesia: subanalysis of the French Aortic National CoreValve and Edwards 2 registry. *Circ Cardiovasc Interv* 2014;7:602-10.
170. Hayek SS, Corrigan FE III, Condado JF, Lin S, Howell S, MacNamara JP, et al. Paravalvular regurgitation after transcatheter aortic valve replacement: comparing transthoracic versus transesophageal echocardiographic guidance. *J Am Soc Echocardiogr* 2017;30:533-40.
171. Bagur R, Rodes-Cabau J, Doyle D, De Laroche R, Villeneuve J, Lemieux J, et al. Usefulness of TEE as the primary imaging technique to guide transcatheter aortic valve implantation. *J Am Coll Cardiol Img* 2011;4:115-24.
172. Ferrari E, Sulzer C, Marcucci C, Rizzo E, Tozzi P, von Segesser LK. Transapical aortic valve implantation without angiography: proof of concept. *Ann Thorac Surg* 2010;89:1925-32.
173. Greason KL, Pochettino A, Sandhu GS, King KS, Holmes DR. Transfemoral transcatheter aortic valve insertion-related intraoperative morbidity: implications of the minimalist approach. *J Thorac Cardiovasc Surg* 2016;151:1026-9.
174. Marcantuono R, Gutsche J, Burke-Julien M, Anwaruddin S, Augoustides JG, Jones D, et al. Rationale, development, implementation, and initial results of a fast track protocol for transfemoral transcatheter aortic valve replacement (TAVR). *Catheter Cardiovasc Interv* 2015;85:648-54.
175. de Brito FS Jr., Carvalho LA, Sarmiento-Leite R, Mangione JA, Lemos P, Siciliano A, et al. Outcomes and predictors of mortality after transcatheter aortic valve implantation: results of the Brazilian registry. *Catheter Cardiovasc Inter* 2015;85:E153-62.
176. Greif M, Lange P, Nabauer M, Schwarz F, Becker C, Schmitz C, et al. Transcatheter aortic valve replacement with the Edwards SAPIEN XT and Medtronic CoreValve prosthesis under fluoroscopic guidance and local anaesthesia only. *Heart* 2014;100:691-5.
177. Holmes DR Jr., Nishimura RA, Grover FL, Brindis RG, Carroll JD, Edwards FH, et al. Annual outcomes with transcatheter valve therapy: from the STS/ACC TVT registry. *J Am Coll Cardiol* 2015;66:2813-23.
178. Dall'Ara G, Eltchaninoff H, Moat N, Laroche C, Goicolea J, Ussia GP, et al. Local and general anaesthesia do not influence outcome of transfemoral aortic valve implantation. *Int J Cardiol* 2014;177:448-54.
179. Condado JF, Haider MN, Lerakis S, Keegan P, Caughron H, Thourani VH, et al. Does minimalist transfemoral transcatheter aortic valve replacement produce better survival in patients with severe chronic obstructive pulmonary disease? *Catheter Cardiovasc Interv* 2017;89:775-80.
180. Jensen HA, Condado JF, Devireddy C, Binongo J, Leshnowar BC, Babaliaros V, et al. Minimalist transcatheter aortic valve replacement: the new standard for surgeons and cardiologists using transfemoral access? *J Thorac Cardiovasc Surg* 2015;150:833-9.
181. Shames S, Koczo A, Hahn R, Gillam LD. In-Stent Flow Acceleration in the SAPIEN transcatheter aortic valve: impact on the echocardiographic assessment of valve function (P3-28). *J Am Soc Echocardiogr* 2011;24:B63.
182. Clavel MA, Rodes-Cabau J, Dumont E, Bagur R, Bergeron S, De Laroche R, et al. Validation and characterization of transcatheter aortic valve effective orifice area measured by Doppler echocardiography. *JACC Cardiovasc Imaging* 2011;4:1053-62.
183. Jilaihawi H, Chin D, Spyt T, Jeilan M, Vasa-Nicotera M, Bence J, et al. Prosthesis-patient mismatch after transcatheter aortic valve implantation with the Medtronic-CoreValve bioprosthesis. *Eur Heart J* 2010;31:857-64.

# Did you know?

You can sign up for eTOCs alerts and never miss any **JASE** articles.



Visit **onlinejase.com** today!